

Research Project

Model-based analysis of various marketing options on the german secondary balancing market for a large-scale storage facility

Sebastian Trümper

Born on: 13th September 1990 in Naumburg
Matriculation number: 3631139

20th April 2025

Supervisor

Dr. Hannes Hobbie, Margrit Wicke, Dr. Christoph Zöphel

Abstract

This study addresses the techno-economic evaluation of a large-scale battery storage system in combination with a wind farm, with a particular focus on participation in the German secondary control reserve market. While the wind-generated electricity is marketed via the Day-Ahead market, the battery storage system participates in the secondary reserve market through capacity and energy bids. The analysis is based on extensive time series data, which were generated using statistical methods and integrated into an efficiently designed optimization model implemented in GAMS. The results indicate that, particularly in scenarios characterized by high feed-in volatility from renewable energy sources and a non-constraining balancing capacity market, it is advantageous to maintain available negative battery capacity over extended periods in order to capitalize on potential price peaks.

Table of Contents

Abstract	1
1 Introduction	1
2 Literatur Review	3
3 Methodology	5
3.1 Market Design Descriptions	7
3.1.1 aFFR - Capacity	8
3.1.2 Day Ahead Market	11
3.1.3 aFFR - Energy	12
3.2 Model components	14
3.2.1 Battery & Charging Capabilities	14
3.2.2 Grid Connection	15
3.3 Complete Model	16
3.4 Timeline Simulation and Scenario Selection	23
3.4.1 aFFR - Capacity	23
3.4.2 Day Ahead Market	26
3.4.3 aFFR - Energy	30
3.5 Simplifications	33
4 Results	36
5 Conclusion	40
6 Appendix	42
Bibliography	53

Sets & Variables & Parameters

Abbreviations

Abbreviations	Description
aFRR	automatic Frequency Restoration Reserve (german secondary balance market)
BESS	battery energy storage systems
GAMS	General Algebraic Modeling System
TSO	transmission system operators
CBMP	cross border marginal price
ARIMA	Autoregressive Integrated Moving Average
SARIMA	Seasonal Autoregressive Integrated Moving Average
TBATS	Trigonometric seasonality Box-Cox transformation
<i>RL</i>	ARMA errors Trend Seasonal components
<i>DA</i>	aFFR capacity / seconday capacity balance market
<i>RA</i>	Day Ahead Markt
	aFFR energy / seconday energy balance market

Table 1: Abbreviations Overview

Variables

Variable	Description
Q_{RL}^{in}	Negative quantity bid at RL
Q_{RL}^{out}	Positive quantity bid at RL
Q_{RA}^{inrB}	Negative quantity bid at RA restricted due to RL positive and negative bid
Q_{RA}^{inrl}	Negative quantity bid at RA restricted due to RL negative bid
Q_{RA}^{inrO}	Negative quantity bid at RA restricted due to RL positive bid
Q_{RA}^{inrN}	Negative quantity bid at RA no restrictions
Q_{RA}^{outrB}	Negative quantity bid at RA restricted due to RL positive and negative bid
Q_{RA}^{outrI}	Negative quantity bid at RA restricted due to RL negative bid
Q_{RA}^{outrO}	Negative quantity bid at RA restricted due to RL positive bid
Q_{RA}^{outrN}	Negative quantity bid at RA no restrictions
Q_{DA}^B	Quantity bid at DA restricted due to RL positive and negative bid
Q_{DA}^I	Quantity bid at DA restricted due to RL negative bid
Q_{DA}^O	Quantity bid at DA restricted due to RL positive bid
Q_{DA}^N	Quantity bid at DA no restrictions
Q_{reload}^B	Reload renew. prod. to bat., restr. due to RL positive and negative bid
Q_{reload}^I	Reload renew. prod. to bat., restr. due to RL negative bid
Q_{reload}^O	Reload renew. prod. to bat., restr. due to RL positive bid
Q_{reload}^N	Reload renew. prod. to bat., no restrictions
WP_{WP}^{inrB}	Working point adjustment (in) quantity at RA restricted due to RL positive and negative bid
WP_{WP}^{inrl}	Working point adjustment (in) quantity at RA restricted due to RL negative bid
WP_{WP}^{inrO}	Working point adjustment (in) quantity at RA restricted due to RL positive bid
WP_{WP}^{inrN}	Working point adjustment (in) quantity at RA no restrictions
WP_{WP}^{outrB}	Working point adjustment (out) quantity at RA restricted due to RL positive and negative bid
WP_{WP}^{outrI}	Working point adjustment (out) quantity at RA restricted due to RL negative bid
WP_{WP}^{outrO}	Working point adjustment (out) quantity at RA restricted due to RL positive bid
WP_{WP}^{outrN}	Working point adjustment (out) quantity at RA no restrictions

Table 2: Variable Overview

Sets

Set	Description
$t_{quarter}$	timesteps in 15 min interval
t_{hour}	timesteps in 1h interval
t_{block}	timesteps in 4h interval
S_{RL}	scenarios balancing capacity market
S_{DA}	scenarios day ahead market
S_{RA}	scenarios for balancing energy market

Table 3: Set Overview

Parameter

Parameter	Description
f_{DA}	forecast price day ahead market
f_{RA}	forecast price RA
$parkCap$	total capacity for the renewable generation
$batCap$	maximum capacity of the BESS
$windProfile$	adjustment of the total capacity due to environment conditions
$p(p_{DA})$	probability for price p_{DA}
$p(p_{RA})$	probability for price p_{RA}
r	rate for charge/discharge BESS
a	Access/grid connection point capacity
$w_y^i(s_y^i)$	Probability for scenario of type i (=in/out) at market y
$p_y^i(s_y^i)$	Bid price of type i (=in/out) at market y for scenario s_y^i
p_y^{exp}	expected price for the market y
c_y^i	market clearing price of type i (=in/out) at market y
m	a arbitrary big number
wp_{ger}	german wind profile
wp_{our}	local wind profile
wsf	scaling factor for local wind profile
$strictFactor$	binary Parameter which sets the strictness for the grid connection point constraints

Table 4: Parameter Overview

Preface

This thesis was developed in collaboration with the UKA - Meißen, under the supervision of Dr. Hannes Hobbie. I would like to express my sincere gratitude to all those involved for their time and support throughout the process.

In particular, I extend my heartfelt thanks to Dr. Hannes Hobbie for his guidance and for organizing the framework of this work, as well as to Margrit Wicke and Dr. Christoph Zöphel for generously sharing their time, expertise, and practical insights.

Thank you very much,
Sebastian Trümper

1 Introduction

The accelerating transition towards renewable energy sources presents both opportunities and challenges for modern power systems. However, the inherent variability and limited predictability of renewable generation pose significant threats to grid stability. As a result, the demand for flexible technologies such as battery energy storage systems (BESS) is increasing, to ensure a reliable and resilient energy supply.

In particular, the provision of ancillary services, especially frequency regulation, has emerged as a promising revenue stream for storage technologies. Germany's balancing markets, including the secondary control reserve (aFRR), offer significant potential for battery systems, thanks to their rapid ramping capabilities and high operational availability.

While renewable generators primarily participate in the day-ahead market based on forecasted production, battery storage systems are typically deployed on balancing markets. Operating a BESS in conjunction with a renewable power plant provides several technical and economic advantages.

On the one hand, excess renewable electricity can be used to charge the battery, thereby avoiding market related fees. On the other hand, generation can be time shifted to periods with higher energy prices. Moreover, the battery can be utilized to compensate for forecast errors and thereby avoid market penalties. Furthermore, the co-location of renewable generation and storage in a hybrid system enables operators to diversify their revenue streams by participating in multiple electricity markets simultaneously. Conversely, sharing a single grid connection point can also present drawbacks. For example, commitments made by either the battery or the wind farm might limit the other's ability to participate freely in the market.

However, such joint operation requires advanced optimization techniques that account for market mechanisms, physical constraints, and operational synergies. In this context, mathematical programming tools such as GAMS (General Algebraic Modeling System) are well-suited to model and solve complex multi-market dispatch problems.

The objective of this study is to determine an optimal bidding strategy for a battery energy storage system co-located with a wind farm, across three relevant electricity markets. These include the day-ahead market, the balancing capacity market, and the balancing energy market.

In practice, this requires a sequence of interdependent decisions: first, the submission of a capacity bid in the balancing market; second, participation in the day-ahead energy market; and finally, submission of an energy bid in the balancing energy market.

This paper presents an optimization model developed in GAMS to simulate the joint operation of a wind farm and a co-located battery storage system. While the wind farm's revenue is derived from the German day-ahead electricity market, the battery system participates in the secondary balancing market.

The model aims to maximize total system profit while respecting both market rules and technical constraints. To this end, synthetic time series data were generated for each market using statistical methods. Representative scenarios were then selected and implemented into the GAMS model to compute an optimal bidding strategy for the storage system.

The next chapter provides a brief overview of the current state of research. Chapter 4 describes the applied methodology in detail, including the general modeling framework and the individual components of the optimization model. Additionally, the process of generating market time series and selecting representative scenarios is discussed. Chapter 5 presents the results, followed by a summary and conclusion in Chapter 6.

2 Literatur Review

There is a wide range of research focused on optimization in individual energy markets. The optimization models used vary greatly. They differ with respect to the markets considered as marketing options, the modeling approaches applied, the data used, and often they focus solely on optimizing battery storage systems or a renewable power plant.

Many models consider only individual markets. Olk et al. [3] consider only the secondary german balancing market and optimize the battery in this context . Cai et al. [1] propose an optimization for a battery combined with an wind park, but focus on the revenue from the park at the day ahead market and use the battery to avoid penalties due to prediction errors.

A core challenge in developing such models lies in how to represent the uncertainty that is inherently present in real-world operations. For example, models that assume perfect foresight and rely on exact historical data are capable of calculating the theoretical maximum return for the system under consideration. But, such models fail to reflect the uncertainty and operational risks that decision-makers face in practice, which limits the applicability of the resulting strategies.

To better address this issue, two methodological approaches are commonly used: Either the model's knowledge of future events is restricted, or the data is modified to represent the uncertainty. For instance Nitsch et al. [4] modeled an optimization problem with perfect foresight but predicted data. Such data could include forecast values that represent expected values or scenario-based data with associated probabilities of occurrence, as discussed by Krishnamurthy et al. [2]. While this approach is useful for representing uncertainty, obtaining suitable data can be very challenging, especially for markets that are highly volatile and influenced by many factors. This is particularly true for the secondary balancing energy market, where energy is traded at short notice to maintain grid stability. OConnor et al. [5] also address the difficulty of predicting prices in balancing energy markets . They demonstrate that even with highly sophisticated models, forecasting balancing prices remains a significant challenge. In the present case, this becomes especially critical since initial bids must be submitted the day before at a time when it is extremely difficult to predict the exact grid status at any given moment the next day. As a result, it is unclear what kind of balancing energy will be required

at that time.

Moreover, much of the existing literature either does not reflect current market regulation or fails to consider the joint operation of all components relevant to this work: a battery energy storage system (BESS), a renewable generator, participation in the Day-Ahead (DA) market, and the provision of automatic frequency restoration reserve (aFRR).

The core challenge of this thesis lies in combining existing modeling approaches for each of these individual components into a single, cohesive optimization model. This integration involves three major difficulties:

- **Model compatibility:** The chosen modeling approaches and data structures for the individual submarkets must be technically compatible with one another.
- **Managing complexity:** Although each subproblem can be solved independently, the overall complexity increases exponentially when combining multiple markets and decision levels. Therefore, simplifications are necessary to maintain computational feasibility without losing essential system dynamics.
- **Data integration/timeline prediction:** The aforementioned points also apply to the integration of time series data. Forecasting and scenario generation must be harmonized across all submarkets to ensure realistic and consistent input for the optimization model.

These challenges affect not only the conceptual design of the model but also its practical implementation and runtime performance. Accordingly, a key contribution of this work is the development of a simplified yet representative optimization framework that integrates these components into a tractable form. Unlike many previous studies, this work focuses on the joint optimization of multiple markets and system components, while implementing scenario-based forecasting data to better represent operational uncertainty.

3 Methodology

The objective of the model is to optimize the marketing of a battery storage system in combination with a wind farm in the simplest way possible. There are various approaches to modeling this. The battery storage system is marketed on the secondary capacity & energy balancing markets, while the wind farm is offered on the Day-Ahead market. The challenge is to connect all three markets without introducing excessive complexity that would limit computational feasibility. In addition, physical characteristics must be taken into account. In particular, both the battery system and the grid connection point must be accurately represented with respect to their key technical properties. The following section outlines the overall modeling approach. First, the general structure and logic of the market models are presented (see Section 3.1). Subsequently, the individual market models are described in detail, highlighting the specific regulations and formulations applied to each market.

Subsequently, the individual structural components are examined in greater detail, with a focus on the specific constraints and modifications they introduce (see Section 3.2).

Finally, the integration of these subparts into a unified optimization framework is explained, including the mechanisms used to ensure consistency across the different market layers (see Section 3.3).

This is followed by a description of how the relevant time series data were generated for each of the considered electricity markets (see Section 3.4).

Finally, the chapter concludes with a discussion of the key simplifications implemented to ensure computational feasibility of the model (see Section 3.5).

3.1 Market Design Descriptions

The model is capable of submitting bids on three markets. Each bid consists of an amount and a corresponding price. The bidding process starts on the secondary balance market with capacity bid, followed by the Day-Ahead market, and finally on the secondary balancing market again with an energy bid.

The goal is to maximize the overall profit, which is composed of the amount and the price. The amount represents the quantity offered on the market, and the price is the price at which the quantity is offered.

The resulting revenue is then given by the following equation:

$$\text{Revenue} = \text{Quantity} * \text{price}$$

In combination with our stochastic approach, a probability (ω) is added. This probability is always interpreted in relation to the associated market price. While the underlying concept remains consistent, the specific interpretation of these probabilities varies slightly across the different markets and is discussed in detail in the respective sections. The expected revenue is calculated as the sum of all possibilities:

$$\text{Revenue} = \sum_{\text{price}} \text{Quantity(price)} * \text{price} * \omega(\text{price}) \quad (3.1)$$

The different prices are represented as different scenarios. Quantity bids can be submitted separately for each scenario, but the total sum of the quantity bids across all scenarios is constrained. An example of scenarios and their associated probabilities can be found in Table 3.1. In this case, the probability would indicate the likelihood that the bid at the corresponding price will be accepted. This approach allows us to independently determine which quantities are allocated to each scenario.

Scenario s	Price p	Probability $\omega(s)$
s1	90	0.6
s2	100	0.5
s3	110	0.4

Table 3.1: Example Scenario Data Table

The objective function to be optimized for this example is as follows:

$$\max Profit = \sum_s Q(s) * p(s) * \omega(s) \quad (3.2)$$

$$0 \leq \sum_s Q(s) \leq q_{max} \quad (3.3)$$

In the following chapters, the individual markets will first be described separately from subsection 3.1.1 to subsection 3.1.3. Subsequently, the transition from individual market problems to an overall decision will be explained [section 3.3].

3.1.1 aFFR - Capacity

General Description

The aFFR market in Germany is divided into two parts: the capacity and the energy market. On the capacity market, bids for the provision of positive or negative balancing capacity are made for a 4-hour time window on the following day. The auction closes at 9 a.m. on the previous day. The settlement is made in [(Euro/MW)/h], and the paid price corresponds to the submitted bid price ("Pay-as-bid" method) [[9]]. Whether our bid is accepted depends directly on the bid price we submit. Since we can determine the price at which we offer capacity on the market, we have a direct influence on the likelihood of our bid being accepted. As a result, we can actively shape the probabilities of the respective scenarios, specifically whether a bid is accepted or rejected.

In the case of a successful bid for capacity, bids must also be placed on the Balancing Energy Market for the same period. The minimum bid quantity is 1 MW, and pre-qualification is required to participate.

Model Implementation

For the Frequency Control Market, the following objective function arises:

$$\max Profit_{RL} = Q_{RL} * p_{RL} * \omega_{RL}(p_{RL}) \quad \forall t_{block} \quad (3.4)$$

By transforming this into a scenario-dependent problem, the following equation results:

$$\max Profit_{RL} = \sum_{t_{block}, S_{RL}} Q_{RL}(t_{block}, S_{RL}) * p_{RL}(t_{block}, S_{RL}) * \omega_{RL}(t_{block}, S_{RL}) \quad (3.5)$$

It should be noted that the quantity is now also scenario-dependent, meaning bids could theoretically be made separately for each assumed scenario. In practice, this is not assumed, as the optimization algorithm will always assign the quantity on the most promising price-acceptance-probability combination. Thus, the quantity serves as an abstract binary activation variable for the different price scenarios.

It should also be noted that both positive (out) and negative (in) capacity bids can be placed. The distinction of accepted and rejected bids is determined by the probabilities ω and $1 - \omega$. While this step is not strictly necessary at this point, it simplifies the later integration of the other markets.

(3.6)

$$maxProfit_{RL} =$$

accepted RL in & out:

$$\begin{aligned} & + \sum_{S_{RL}^{out}} \sum_{S_{RL}^{in}} (\omega_{RL}^{in}(t_{block}, S_{RL}^{in}) * \omega_{RL}^{out}(t_{block}, S_{RL}^{out})) * (\\ & + (Q_{RL}^{in}(t_{block}, S_{RL}^{in}) * p_{RL}^{in}(t_{block}, S_{RL}^{in})) \\ & + (Q_{RL}^{out}(t_{block}, S_{RL}^{out}) * p_{RL}^{out}(t_{block}, S_{RL}^{out})) \end{aligned}$$

accepted RL in & declined out:

$$\begin{aligned} & + \sum_{S_{RL}^{out}} \sum_{S_{RL}^{in}} (\omega_{RL}^{in}(t_{block}, S_{RL}^{in}) * (1 - \omega_{RL}^{out}(t_{block}, S_{RL}^{out}))) * (\\ & + (Q_{RL}^{in}(t_{block}, S_{RL}^{in}) * p_{RL}^{in}(t_{block}, S_{RL}^{in})) \end{aligned}$$

declined RL in & accepted out:

$$\begin{aligned} & + \sum_{S_{RL}^{out}} \sum_{S_{RL}^{in}} ((1 - \omega_{RL}^{in}(t_{block}, S_{RL}^{in})) * \omega_{RL}^{out}(t_{block}, S_{RL}^{out})) * (\\ & + (Q_{RL}^{out}(t_{block}, S_{RL}^{out}) * p_{RL}^{out}(t_{block}, S_{RL}^{out})) \end{aligned}$$

(3.7)

$$\forall t_{hour} = \left\lfloor \frac{t_{quarter}}{4} \right\rfloor, t_{block} = \left\lfloor \frac{t_{quarter}}{16} \right\rfloor$$

The constraints 3.8 ensure that the offered quantities are not negative. Additionally, it is ensured that the connection capacity a is not exceeded (equation 3.10), and that the battery is capable of handling the corresponding power demand (equation 3.9).

It is also important that the battery storage state can fulfill the offered power within the respective time window 3.11 & 3.12. Note that the offered capacity is specified per hour, while the battery storage is calculated in 15-minute intervals. Therefore, the offered capacity must be multiplied by 0.25 to obtain the value for the quarter-hour interval.

For example, if 100 MW are offered in the secondary balancing market, then for each quarter-hour in the corresponding block, 25 MWh of positive or negative work must be reserved.

$$0 \leq Q_{RL}^{in}(t_{block}, s_{RL}^{in}), Q_{RL}^{out}(t_{block}, s_{RL}^{out}) \quad \forall s_{RL}^{in}, s_{RL}^{out} \quad (3.8)$$

$$r \geq \sum_{s_{RL}^{in}} Q_{RL}^{in}(t_{block}, s_{RL}^{in}), \sum_{s_{RL}^{out}} Q_{RL}^{out}(t_{block}, s_{RL}^{out}) \quad (3.9)$$

$$a + \sum_{s_{RL}^{in}} Q_{RL}^{in}(t_{block}, s_{RL}^{in}) \geq \sum_{s_{RL}^{out}} Q_{RL}^{out}(t_{block}, s_{RL}^{out}) \quad (3.10)$$

$$Q_{RL}^{in}(t_{block}, s_{RL}^{in}) * 0.25 \leq batCap - BatStat(t_{quarter, s_{RA}}) \quad \forall t_{block} = \left\lfloor \frac{t_{quarter}}{16} \right\rfloor \quad (3.11)$$

$$Q_{RL}^{out}(t_{block}, s_{RL}^{out}) * 0.25 \leq BatStat(t_{quarter, s_{RA}}) \quad \forall t_{block} = \left\lfloor \frac{t_{quarter}}{16} \right\rfloor \quad (3.12)$$

3.1.2 Day Ahead Market

General Description

The wind park is marketed in the Day-Ahead Market (DA). Here, bids are made for 1-hour intervals on the following day. The auction closes at 12:00 PM the day before. The minimum bid quantity is 0.1 MWh, and bids between -500 Euros and 3000 Euros are accepted. The settlement is in [Euro/MWh], and the price is determined using the "Pay-as-cleared" method. This means that all participants receive the price of the highest accepted bid.

Model Implementation

In parallel with the previous chapter, the equations for the Day-Ahead Market (DA) are derived. The Day-Ahead Market is the platform where the electricity from the wind farm is marketed. Consequently, there are no positive and negative bids. As the operator of the wind farm, we have operating costs that are close to zero, allowing us to offer electricity at a very low price. In practice, this means that we are almost free to decide whether or not to sell electricity on the day-ahead market and receive the clearing price. The probability $\omega_{DA}(t_{hour}, s_{DA})$ indicates the probability for the corresponding price $p(t_{hour}, s_{DA})$. The expected profit is thus calculated as follows:

$$\max_{Q_{DA}(t_{hour}, s_{DA})} Profit_{DA} = \sum_{t_{hour}} Q_{DA}(t_{hour}) * \sum_{t_{hour}, s_{DA}} p(t_{hour}, s_{DA}) * \omega_{DA}(t_{hour}, s_{DA}) \quad (3.13)$$

$$\rightarrow \max_{Q_{DA}(t_{hour}, s_{DA})} Profit_{DA} = \sum_{t_{hour}} Q_{DA}(t_{hour}) * p_{DA}^{exp}(t_{hour}) \quad (3.14)$$

It is important to note that the amount of electricity generated by the wind park cannot be freely chosen. Rather, it is constrained by the prevailing weather conditions (equation 3.16). In addition, we have the option to store the generated electricity instead of feeding it into the grid, thus allowing the battery to be recharged (equation 3.16).

$$0 \leq Q_{DA}(t_{hour}, s_{DA}) \quad \forall t_{hour}, s_{DA} \quad (3.15)$$

$$Q_{DA}(t_{hour}) \leq parkCap * windProfile(t_{hour}) - Q_{reload}(t_{hour}) \quad \forall t_{hour} \quad (3.16)$$

$$Q_{DA}(t_{hour}) \leq a \quad \forall t_{hour} \quad (3.17)$$

3.1.3 aFFR - Energy

General Description

In the secondary reserve energy market, bids are placed for 15-minute intervals. The auction closes 25 minutes before the start of the associated 15-minute block. Each prequalified participant is allowed to bid on this market, regardless of whether a bid has been successful in the aFFR capacity market. If a bid has been accepted in the aFFR capacity market, a bid must also be made for the corresponding time window in the secondary market. Payment is made only for the actual energy delivered. The dispatch of energy is based on the merit-order list, from the cheapest to the most expensive supplier. With a high offered energy price, the likelihood of the offered energy being called decreases. This is a "Pay-as-cleared" market, meaning all participants receive the price of the last accepted bid. Since Germany's entry into the PICASSO network, the marginal price corresponds to the cross-border marginal price (CBMP) [6].

Model Implementation

In parallel to the aFFR capacity market, the aFFR energy market is constructed (equation 3.18). Since we cannot precisely predict the state of the electricity market on the following day, multiple possible scenarios are considered, all of which are assumed to be equally likely (for more details, see Chapter 3.4.3). This applies to both positive (out) and negative (in) balancing energy.

$$\maxProfit = \sum_{t_{quarter}} \left[\sum_{S_{RA}} 1/|S_{RA}| * p_{RA}^{in}(t_{quarter}, S_{RA}) * Q_{RA}^{in}(t_{quarter}, S_{RA}) + \sum_{S_{RA}} 1/|S_{RA}| * p_{RA}^{out}(t_{quarter}, S_{RA}) * Q_{RA}^{out}(t_{quarter}, S_{RA}) \right] \quad (3.18)$$

The energy is also subject to several constraints. Specifically, the battery storage must be able to deliver the required work (equation 3.19 - 3.22), and the connection point must have sufficient capacity (equation 3.23 & 3.24).

$$\sum_{S_{RA}} Q_{RA}^{out}(t_{quarter}, S_{RA}) \leq r/4 \quad \forall S_{RA}, t_{quarter} \quad (3.19)$$

$$\sum_{S_{RA}} Q_{RA}^{in}(t_{quarter}, S_{RA}) \leq r/4 \quad \forall S_{RA}, t_{quarter} \quad (3.20)$$

$$\sum_{S_{RA}} Q_{RA}^{out}(t_{quarter}, S_{RA}) \leq BatStat(t_{quarter}, S_{RA}) \quad \forall S_{RA}, t_{quarter} \quad (3.21)$$

$$\sum_{S_{RA}} Q_{RA}^{in}(t_{quarter}, S_{RA}) \leq batCap - BatStat(t_{quarter}, S_{RA}) \quad \forall S_{RA}, t_{quarter} \quad (3.22)$$

$$\sum_{S_{RA}} Q_{RA}^{out}(t_{quarter}, S_{RA}) \leq a/4 \quad \forall S_{RA}, t_{quarter} \quad (3.23)$$

$$\sum_{S_{RA}} Q_{RA}^{in}(t_{quarter}, S_{RA}) \leq a/4 \quad \forall S_{RA}, t_{quarter} \quad (3.24)$$

3.2 Model components

The previous presented equations served to calculate the profit to be maximized. But, there are fundamental real-world components that must be reflected in our model, which impose constraints on the profit-maximizing formulations.

We begin by examining the battery system and its charging capabilities in more detail. Subsequently, the modeling of the grid connection point is discussed.

3.2.1 Battery & Charging Capabilities

The fundamental properties of the battery storage are described through parameters combined with constraints. The battery storage has a maximum charging and discharging rate r and a maximum capacity $batCap$. The battery status $BatStat$ is recalculated every quarter-hour and can be found in equation 3.25. Since the recharge amount Q_{reload} , which comes from the wind park, is calculated hourly, it must be converted to quarter-hourly values. The battery status for the timestep $t_{quarter} + 1$ is derived from the battery status at the previous timestep $t_{quarter}$, along with the actual negative reserve energy delivered, minus the actual positive reserve energy delivered. Furthermore, there is the option for a working point adjustment WP . This adjustment can be made to align the battery's charge level with the obligations that need to be met.

$$\begin{aligned} BatStat(t_{quarter} + 1) = & BatStat(t_{quarter}) + \frac{1}{4} Q_{reload}(t_{hour}) \\ & + \sum_{SRA} 1/|SRA| * Q_{RA}^{in}(t_{quarter}, SRA) \\ & - \sum_{SRA} 1/|SRA| * Q_{RA}^{out}(t_{quarter}, SRA) \\ & - \sum_{SRA} 1/|SRA| * WP_{out}(t_{quarter}, SRA) \\ & + \sum_{SRA} 1/|SRA| * WP_{in}(t_{quarter}, SRA) \\ & \forall t_{quarter}, t_{hour} = \left\lfloor \frac{t_{quarter}}{4} \right\rfloor \end{aligned} \quad (3.25)$$

$$0 \leq BatStat(t_{quarter}) \quad (3.26)$$

$$BatStat(t_{quarter}) \leq batCap \quad (3.27)$$

3.2.2 Grid Connection

The wind farm and the battery storage system share a common grid connection. As a result, their combined output is subject to a maximum power constraint, which must be respected throughout the optimization process. The maximum power that can flow through the connection point is a . This power limit applies in both directions, as shown in equations 3.28 and 3.29. Since this constraint applies to all quarter-hour intervals, we have to divide the work of the wind farm and the grid connection maximum power by four. The *strictFactor* describes a binary parameter that can be set to either 0 or 1. When set to 0, the parameter is considered active, meaning that power contributions in the opposite direction do not relax the corresponding constraint. For subsequent calculations, this factor is always assumed to be active.

$$\begin{aligned} & \frac{a}{4} + \text{strictFactor} * (Q_{RA}^{in}(t_{quarter}, S_{RA}) + WP_{in}(t_{quarter}, S_{RA})) \\ & \geq \frac{1}{4} Q_{DA}(t_{hour}) + Q_{RA}^{out}(t_{quarter}, S_{RA}) + WP_{out}(t_{quarter}, S_{RA}) \\ & \forall S_{RA}, t_{quarter}, t_{hour} = \left\lfloor \frac{t_{quarter}}{4} \right\rfloor \end{aligned} \quad (3.28)$$

$$\begin{aligned} & \frac{a}{4} + \text{strictFactor} * (\frac{1}{4} Q_{DA}(t_{hour}) + Q_{RA}^{out}(t_{quarter}, S_{RA}) + WP_{out}(t_{quarter}, S_{RA})) \\ & \geq Q_{RA}^{in}(t_{quarter}, S_{RA}) + WP_{in}(t_{quarter}, S_{RA}) \\ & \forall S_{RA}, t_{quarter}, t_{hour} = \left\lfloor \frac{t_{quarter}}{4} \right\rfloor \end{aligned} \quad (3.29)$$

3.3 Complete Model

In order to integrate everything into a comprehensive model, several adjustments need to be made. Firstly, the aFFR capacity market is closed in advance, meaning that when the decision for the DA market is made, the outcome of the aFFR capacity market is already known. This implies that the variables in the subsequent markets can be planned with consideration of the various possible outcomes.

To enable this, all the following variables are split into the 4 basic scenarios. These scenarios are:

1. accepted positive and negative balance capacity bid → $Variable^{rB}$
2. accepted positive and declined negative balance capacity bid → $Variable^{rO}$
3. declined positives and accepted negative balance capacity bid → $Variable^{rl}$
4. declined positives and negative balance capacity bid → $Variable^{rN}$

This approach helps avoid dimensionality per variable and reduces the complexity of the base model. But, in order to consider all fundamental capacity price options (scenarios) and their subsequent planning across all variables, the dimensions of the variables Q_{DA} , Q_{RA}^{out} , and Q_{RA}^{in} are expanded by the dimensions of s_{RL}^{out} and s_{RL}^{in} . The resulting, split and higher-dimensional objective functions of the subsequent markets are then incorporated into the maximization profit equation of the initial decision in the aFFR capacity market [3.30]. Additionally, the hourly revenue calculations from the aFFR capacity market and the day-ahead market need to be adjusted for the quarter-hourly calculations.

$$\begin{aligned}
 \max Profit = & -workingCosts + \sum_{t_{quarter}} \\
 \text{accepted RL in \& out:} & + \sum_{S_{RL}^{out}} \sum_{S_{RL}^{in}} (\omega_{RL}^{in}(t_{block}, S_{RL}^{in}) * \omega_{RL}^{out}(t_{block}, S_{RL}^{out})) * \\
 & + (\frac{1}{4} * (Q_{RL}^{in}(t_{block}, S_{RL}^{in}) * p_{RL}^{in}(t_{block}, S_{RL}^{in}))) \\
 & + (\frac{1}{4} * (Q_{RL}^{out}(t_{block}, S_{RL}^{out}) * p_{RL}^{out}(t_{block}, S_{RL}^{out}))) \\
 & + (\frac{1}{4} * (Q_{DA}^{rB}(t_{hour}, S_{RL}^{in}, S_{RL}^{out}) * p_{DA}^{exp}(t_{hour}))) \\
 & + (\sum_{S_{RA}} 1 / |S_{RA}| * p_{RA}^{in}(t_{quarter}, S_{RA}) * Q_{RA}^{inrB}(t_{quarter}, S_{RA}, S_{RL}^{in}, S_{RL}^{out})) \\
 & + (\sum_{S_{RA}} 1 / |S_{RA}| * p_{RA}^{out}(t_{quarter}, S_{RA}) * Q_{RA}^{outrB}(t_{quarter}, S_{RA}, S_{RL}^{in}, S_{RL}^{out})) \\
 \text{accepted RL in \& declined out:} & + \sum_{S_{RL}^{out}} \sum_{S_{RL}^{in}} (\omega_{RL}^{in}(t_{block}, S_{RL}^{in}) * (1 - \omega_{RL}^{out}(t_{block}, S_{RL}^{out}))) * \\
 & + (\frac{1}{4} * (Q_{RL}^{in}(t_{block}, S_{RL}^{in}) * p_{RL}^{in}(t_{block}, S_{RL}^{in}))) \\
 & + (\frac{1}{4} * (Q_{DA}^{rl}(t_{hour}, S_{RL}^{in}, S_{RL}^{out}) * p_{DA}^{exp}(t_{hour}))) \\
 & + (\sum_{S_{RA}} 1 / |S_{RA}| * p_{RA}^{in}(t_{quarter}, S_{RA}) * Q_{RA}^{inrl}(t_{quarter}, S_{RA}, S_{RL}^{in}, S_{RL}^{out})) \\
 & + (\sum_{S_{RA}} 1 / |S_{RA}| * p_{RA}^{out}(t_{quarter}, S_{RA}) * Q_{RA}^{outrl}(t_{quarter}, S_{RA}, S_{RL}^{in}, S_{RL}^{out})) \\
 \text{declined RL in \& accepted out:} & + \sum_{S_{RL}^{out}} \sum_{S_{RL}^{in}} ((1 - \omega_{RL}^{in}(t_{block}, S_{RL}^{in})) * \omega_{RL}^{out}(t_{block}, S_{RL}^{out})) * \\
 & + (\frac{1}{4} * (Q_{RL}^{out}(t_{block}, S_{RL}^{out}) * p_{RL}^{out}(t_{block}, S_{RL}^{out}))) \\
 & + (\frac{1}{4} * (Q_{DA}^{rO}(t_{hour}, S_{RL}^{in}, S_{RL}^{out}) * p_{DA}^{exp}(t_{hour}))) \\
 & + (\sum_{S_{RA}} 1 / |S_{RA}| * p_{RA}^{in}(t_{quarter}, S_{RA}) * Q_{RA}^{inrO}(t_{quarter}, S_{RA}, S_{RL}^{in}, S_{RL}^{out})) \\
 & + (\sum_{S_{RA}} 1 / |S_{RA}| * p_{RA}^{out}(t_{quarter}, S_{RA}) * Q_{RA}^{outrO}(t_{quarter}, S_{RA}, S_{RL}^{in}, S_{RL}^{out})) \\
 \text{declined RL in \& out:} & + \sum_{S_{RL}^{out}} \sum_{S_{RL}^{in}} ((1 - (\omega_{RL}^{in}(t_{block}, S_{RL}^{in}))) * (1 - \omega_{RL}^{out}(t_{block}, S_{RL}^{out}))) * \\
 & + (\frac{1}{4} * (Q_{DA}^{rN}(t_{hour}, S_{RL}^{in}, S_{RL}^{out}) * p_{DA}^{exp}(t_{hour}))) \\
 & + (\sum_{S_{RA}} 1 / |S_{RA}| * p_{RA}^{in}(t_{quarter}, S_{RA}) * Q_{RA}^{inrN}(t_{quarter}, S_{RA}, S_{RL}^{in}, S_{RL}^{out})) \\
 & + (\sum_{S_{RA}} 1 / |S_{RA}| * p_{RA}^{out}(t_{quarter}, S_{RA}) * Q_{RA}^{outrN}(t_{quarter}, S_{RA}, S_{RL}^{in}, S_{RL}^{out})) \\
 & \forall t_{hour} = \left\lfloor \frac{t_{quarter}}{4} \right\rfloor, t_{block} = \left\lfloor \frac{t_{quarter}}{16} \right\rfloor, S_{RA}
 \end{aligned} \tag{3.30}$$

The costs in this context arise from the working point adjustments. The expected working point costs are derived from the opposite market price of the aFFR energy market, factored by a working point factor WPF . This assumption is based on the idea that, for example, if I want to spontaneously release energy, someone else must be willing to absorb this energy in return. In other words, when we have a positive energy output, we compensate for the provision of negative energy by another party. The price for this negative energy provision is derived from the price of the negative energy balance market, adjusted by the working point factor due to its urgency[3.31].

$$workingCosts = \sum_{t_{quarter}}$$

accepted RL in & out:

$$\begin{aligned} & \sum_{S_{RL}^{out}} \sum_{S_{RL}^{in}} (\omega_{RL}^{in}(t_{block}, S_{RL}^{in}) * \omega_{RL}^{out}(t_{block}, S_{RL}^{out})) * (\\ & + \sum_{S_{RA}} WP_{RA}^{inrB}(t_{quarter}, S_{RA}, S_{RL}^{in}, S_{RL}^{out}) * p_{ER}^{in} * WPF * 1 / |S_{RA}|) \\ & + \sum_{S_{RA}} WP_{RA}^{outrB}(t_{quarter}, S_{RA}, S_{RL}^{in}, S_{RL}^{out}) * p_{ER}^{in} * WPF * 1 / |S_{RA}| \end{aligned}$$

accepted RL in & declined out:

$$\begin{aligned} & + \sum_{S_{RL}^{out}} \sum_{S_{RL}^{in}} (\omega_{RL}^{in}(t_{block}, S_{RL}^{in}) * (1 - \omega_{RL}^{out}(t_{block}, S_{RL}^{out}))) * (\\ & + \sum_{S_{RA}} WP_{RA}^{inrl}(t_{quarter}, S_{RA}, S_{RL}^{in}, S_{RL}^{out}) * p_{ER}^{in} * WPF * 1 / |S_{RA}|) \\ & + \sum_{S_{RA}} WP_{RA}^{outrl}(t_{quarter}, S_{RA}, S_{RL}^{in}, S_{RL}^{out}) * p_{ER}^{in} * WPF * 1 / |S_{RA}| \end{aligned}$$

declined RL in & accepted out:

$$\begin{aligned} & + \sum_{S_{RL}^{out}} \sum_{S_{RL}^{in}} ((1 - \omega_{RL}^{in}(t_{block}, S_{RL}^{in})) * \omega_{RL}^{out}(t_{block}, S_{RL}^{out})) * (\\ & + \sum_{S_{RA}} WP_{RA}^{inrO}(t_{quarter}, S_{RA}, S_{RL}^{in}, S_{RL}^{out}) * p_{ER}^{in} * WPF * 1 / |S_{RA}|) \\ & + \sum_{S_{RA}} WP_{RA}^{outrO}(t_{quarter}, S_{RA}, S_{RL}^{in}, S_{RL}^{out}) * p_{ER}^{in} * WPF * 1 / |S_{RA}| \end{aligned}$$

declined RL in & out:

$$\begin{aligned} & + \sum_{S_{RL}^{out}} \sum_{S_{RL}^{in}} ((1 - (\omega_{RL}^{in}(t_{block}, S_{RL}^{in}) * (1 - \omega_{RL}^{out}(t_{block}, S_{RL}^{out})))) * (\\ & + \sum_{S_{RA}} WP_{RA}^{inrN}(t_{quarter}, S_{RA}, S_{RL}^{in}, S_{RL}^{out}) * p_{ER}^{in} * WPF * 1 / |S_{RA}|) \\ & + \sum_{S_{RA}} WP_{RA}^{outrN}(t_{quarter}, S_{RA}, S_{RL}^{in}, S_{RL}^{out}) * p_{ER}^{in} * WPF * 1 / |S_{RA}|) \\ & \forall t_{hour} = \left\lfloor \frac{t_{quarter}}{4} \right\rfloor, t_{block} = \left\lfloor \frac{t_{quarter}}{16} \right\rfloor \end{aligned}$$

(3.31)

The calculation of the battery storage status is then given by the following overall equation:

$$BatStat(t_{quarter, S_{RA}} + 1) = BatStat(t_{quarter, S_{RA}})$$

accepted RL in & out:

$$\begin{aligned} &+ \sum_{S_{RL}^{out}} \sum_{S_{RL}^{in}} (\omega_{RL}^{in}(t_{block}, S_{RL}^{in}) * \omega_{RL}^{out}(t_{block}, S_{RL}^{out})) * (\\ &+ Q_{reload}^B(t_{hour}, S_{RL}^{in}, S_{RL}^{out})/4) \\ &+ (WP_{RA}^{inrB}(t_{quarter}, S_{RA}, S_{RL}^{in}, S_{RL}^{out}) + Q_{RA}^{inrB}(t_{quarter}, S_{RA}, S_{RL}^{in}, S_{RL}^{out})) \\ &- (WP_{RA}^{outrB}(t_{quarter}, S_{RA}, S_{RL}^{in}, S_{RL}^{out}) + Q_{RA}^{outrB}(t_{quarter}, S_{RA}, S_{RL}^{in}, S_{RL}^{out})) \end{aligned}$$

accepted RL in & declined out:

$$\begin{aligned} &+ \sum_{S_{RL}^{out}} \sum_{S_{RL}^{in}} (\omega_{RL}^{in}(t_{block}, S_{RL}^{in}) * (1 - \omega_{RL}^{out}(t_{block}, S_{RL}^{out}))) * (\\ &+ Q_{reload}^I(t_{hour}, S_{RL}^{in}, S_{RL}^{out})/4) \\ &+ (WP_{RA}^{inrI}(t_{quarter}, S_{RA}, S_{RL}^{in}, S_{RL}^{out}) + Q_{RA}^{inrI}(t_{quarter}, S_{RA}, S_{RL}^{in}, S_{RL}^{out})) \\ &- (WP_{RA}^{outrI}(t_{quarter}, S_{RA}, S_{RL}^{in}, S_{RL}^{out}) + Q_{RA}^{outrI}(t_{quarter}, S_{RA}, S_{RL}^{in}, S_{RL}^{out})) \end{aligned}$$

declined RL in & accepted out:

$$\begin{aligned} &+ \sum_{S_{RL}^{out}} \sum_{S_{RL}^{in}} ((1 - \omega_{RL}^{in}(t_{block}, S_{RL}^{in})) * \omega_{RL}^{out}(t_{block}, S_{RL}^{out})) * (\\ &+ Q_{reload}^O(t_{hour}, S_{RL}^{in}, S_{RL}^{out})/4) \\ &+ (WP_{RA}^{inrO}(t_{quarter}, S_{RA}, S_{RL}^{in}, S_{RL}^{out}) + Q_{RA}^{inrO}(t_{quarter}, S_{RA}, S_{RL}^{in}, S_{RL}^{out})) \\ &- (WP_{RA}^{outrO}(t_{quarter}, S_{RA}, S_{RL}^{in}, S_{RL}^{out}) + Q_{RA}^{outrO}(t_{quarter}, S_{RA}, S_{RL}^{in}, S_{RL}^{out})) \end{aligned}$$

declined RL in & out:

$$\begin{aligned} &+ \sum_{S_{RL}^{out}} \sum_{S_{RL}^{in}} ((1 - \omega_{RL}^{in}(t_{block}, S_{RL}^{in})) * (1 - \omega_{RL}^{out}(t_{block}, S_{RL}^{out}))) * (\\ &+ Q_{reload}^N(t_{hour}, S_{RL}^{in}, S_{RL}^{out})/4) \\ &+ (WP_{RA}^{inrN}(t_{quarter}, S_{RA}, S_{RL}^{in}, S_{RL}^{out}) + Q_{RA}^{inrN}(t_{quarter}, S_{RA}, S_{RL}^{in}, S_{RL}^{out})) \\ &- (WP_{RA}^{outrN}(t_{quarter}, S_{RA}, S_{RL}^{in}, S_{RL}^{out}) + Q_{RA}^{outrN}(t_{quarter}, S_{RA}, S_{RL}^{in}, S_{RL}^{out})) \end{aligned}$$

$$\forall t_{quarter}, t_{hour} = \left\lfloor \frac{t_{quarter}}{4} \right\rfloor, t_{block} = \left\lfloor \frac{t_{quarter}}{16} \right\rfloor \quad (3.32)$$

The connection point constraints must be defined for all possible outcomes and subsequent variables. Additionally, they must be ensured in both the positive and negative directions as a safeguard.

$$\begin{aligned}
 & \frac{\alpha}{4} + \sum_{S_{RL}^{in}, S_{RL}^{out}} WP_{RA}^{inrB}(t_{quarter}, S_{RA}, S_{RL}^{in}, S_{RL}^{out}) + Q_{RA}^{inrB}(t_{quarter}, S_{RA}, S_{RL}^{in}, S_{RL}^{out}) \\
 & \geq \sum_{S_{DA}, S_{RL}^{in}, S_{RL}^{out}} (Q_{DA}^r(t_{hour}, S_{RL}^{in}, S_{RL}^{out}) * 0.25) \\
 & + \sum_{S_{RL}^{in}, S_{RL}^{out}} WP_{RA}^{outrB}(t_{quarter}, S_{RA}, S_{RL}^{in}, S_{RL}^{out}) + Q_{RA}^{outrB}(t_{quarter}, S_{RA}, S_{RL}^{in}, S_{RL}^{out}) \\
 & \quad \forall t_{quarter}, t_{hour} = \left\lfloor \frac{t_{quarter}}{4} \right\rfloor, t_{block} = \left\lfloor \frac{t_{quarter}}{16} \right\rfloor
 \end{aligned} \tag{3.33}$$

$$\begin{aligned}
 & \frac{\alpha}{4} + \sum_{S_{RL}^{in}, S_{RL}^{out}} WP_{RA}^{inrl}(t_{quarter}, S_{RA}, S_{RL}^{in}, S_{RL}^{out}) + Q_{RA}^{inrl}(t_{quarter}, S_{RA}, S_{RL}^{in}, S_{RL}^{out}) \\
 & \geq \sum_{S_{DA}, S_{RL}^{in}, S_{RL}^{out}} (Q_{DA}^r(t_{hour}, S_{RL}^{in}, S_{RL}^{out}) * 0.25) \\
 & + \sum_{S_{RL}^{in}, S_{RL}^{out}} WP_{RA}^{outrl}(t_{quarter}, S_{RA}, S_{RL}^{in}, S_{RL}^{out}) + Q_{RA}^{outrl}(t_{quarter}, S_{RA}, S_{RL}^{in}, S_{RL}^{out}) \\
 & \quad \forall t_{quarter}, t_{hour} = \left\lfloor \frac{t_{quarter}}{4} \right\rfloor, t_{block} = \left\lfloor \frac{t_{quarter}}{16} \right\rfloor
 \end{aligned} \tag{3.34}$$

$$\begin{aligned}
 & \frac{\alpha}{4} + \sum_{S_{RL}^{in}, S_{RL}^{out}} WP_{RA}^{inrO}(t_{quarter}, S_{RA}, S_{RL}^{in}, S_{RL}^{out}) + Q_{RA}^{inrO}(t_{quarter}, S_{RA}, S_{RL}^{in}, S_{RL}^{out}) \\
 & \geq \sum_{S_{DA}, S_{RL}^{in}, S_{RL}^{out}} (Q_{DA}^r(t_{hour}, S_{RL}^{in}, S_{RL}^{out}) * 0.25) \\
 & + \sum_{S_{RL}^{in}, S_{RL}^{out}} WP_{RA}^{outrO}(t_{quarter}, S_{RA}, S_{RL}^{in}, S_{RL}^{out}) + Q_{RA}^{outrO}(t_{quarter}, S_{RA}, S_{RL}^{in}, S_{RL}^{out}) \\
 & \quad \forall t_{quarter}, t_{hour} = \left\lfloor \frac{t_{quarter}}{4} \right\rfloor, t_{block} = \left\lfloor \frac{t_{quarter}}{16} \right\rfloor
 \end{aligned} \tag{3.35}$$

$$\begin{aligned}
 & \frac{\alpha}{4} + \sum_{S_{RL}^{in}, S_{RL}^{out}} WP_{RA}^{inrN}(t_{quarter}, S_{RA}, S_{RL}^{in}, S_{RL}^{out}) + Q_{RA}^{inrN}(t_{quarter}, S_{RA}, S_{RL}^{in}, S_{RL}^{out}) \\
 & \geq \sum_{S_{DA}, S_{RL}^{in}, S_{RL}^{out}} (Q_{DA}^r(t_{hour}, S_{RL}^{in}, S_{RL}^{out}) * 0.25) \\
 & + \sum_{S_{RL}^{in}, S_{RL}^{out}} WP_{RA}^{outrN}(t_{quarter}, S_{RA}, S_{RL}^{in}, S_{RL}^{out}) + Q_{RA}^{outrN}(t_{quarter}, S_{RA}, S_{RL}^{in}, S_{RL}^{out}) \\
 & \quad \forall t_{quarter}, t_{hour} = \left\lfloor \frac{t_{quarter}}{4} \right\rfloor, t_{block} = \left\lfloor \frac{t_{quarter}}{16} \right\rfloor
 \end{aligned} \tag{3.36}$$

$$\begin{aligned}
 & \frac{\alpha}{4} + \sum_{S_{DA}, S_{RL}^{in}, S_{RL}^{out}} (Q_{DA}^{rB}(t_{hour}, S_{RL}^{in}, S_{RL}^{out}) * 0.25) \\
 & + \sum_{S_{RL}^{in}, S_{RL}^{out}} WP_{RA}^{outrB}(t_{quarter}, S_{RA}, S_{RL}^{in}, S_{RL}^{out}) + Q_{RA}^{outrB}(t_{quarter}, S_{RA}, S_{RL}^{in}, S_{RL}^{out}) \\
 & \geq \sum_{S_{RL}^{in}, S_{RL}^{out}} WP_{RA}^{inrB}(t_{quarter}, S_{RA}, S_{RL}^{in}, S_{RL}^{out}) + Q_{RA}^{inrB}(t_{quarter}, S_{RA}, S_{RL}^{in}, S_{RL}^{out}) \\
 & \quad \forall t_{quarter}, t_{hour} = \left\lfloor \frac{t_{quarter}}{4} \right\rfloor, t_{block} = \left\lfloor \frac{t_{quarter}}{16} \right\rfloor \tag{3.37}
 \end{aligned}$$

$$\begin{aligned}
 & \frac{\alpha}{4} + \sum_{S_{DA}, S_{RL}^{in}, S_{RL}^{out}} (Q_{DA}^{rl}(t_{hour}, S_{RL}^{in}, S_{RL}^{out}) * 0.25) \\
 & + \sum_{S_{RL}^{in}, S_{RL}^{out}} WP_{RA}^{outrl}(t_{quarter}, S_{RA}, S_{RL}^{in}, S_{RL}^{out}) + Q_{RA}^{outrl}(t_{quarter}, S_{RA}, S_{RL}^{in}, S_{RL}^{out}) \\
 & \geq \sum_{S_{RL}^{in}, S_{RL}^{out}} WP_{RA}^{inrl}(t_{quarter}, S_{RA}, S_{RL}^{in}, S_{RL}^{out}) + Q_{RA}^{inrl}(t_{quarter}, S_{RA}, S_{RL}^{in}, S_{RL}^{out}) \\
 & \quad \forall t_{quarter}, t_{hour} = \left\lfloor \frac{t_{quarter}}{4} \right\rfloor, t_{block} = \left\lfloor \frac{t_{quarter}}{16} \right\rfloor \tag{3.38}
 \end{aligned}$$

$$\begin{aligned}
 & \frac{\alpha}{4} + \sum_{S_{DA}, S_{RL}^{in}, S_{RL}^{out}} (Q_{DA}^{rO}(t_{hour}, S_{RL}^{in}, S_{RL}^{out}) * 0.25) \\
 & + \sum_{S_{RL}^{in}, S_{RL}^{out}} WP_{RA}^{outrO}(t_{quarter}, S_{RA}, S_{RL}^{in}, S_{RL}^{out}) + Q_{RA}^{outrO}(t_{quarter}, S_{RA}, S_{RL}^{in}, S_{RL}^{out}) \\
 & \geq \sum_{S_{RL}^{in}, S_{RL}^{out}} WP_{RA}^{inrO}(t_{quarter}, S_{RA}, S_{RL}^{in}, S_{RL}^{out}) + Q_{RA}^{inrO}(t_{quarter}, S_{RA}, S_{RL}^{in}, S_{RL}^{out}) \\
 & \quad \forall t_{quarter}, t_{hour} = \left\lfloor \frac{t_{quarter}}{4} \right\rfloor, t_{block} = \left\lfloor \frac{t_{quarter}}{16} \right\rfloor \tag{3.39}
 \end{aligned}$$

$$\begin{aligned}
 & \frac{\alpha}{4} + \sum_{S_{DA}, S_{RL}^{in}, S_{RL}^{out}} (Q_{DA}^{rN}(t_{hour}, S_{RL}^{in}, S_{RL}^{out}) * 0.25) \\
 & + \sum_{S_{RL}^{in}, S_{RL}^{out}} WP_{RA}^{outrN}(t_{quarter}, S_{RA}, S_{RL}^{in}, S_{RL}^{out}) + Q_{RA}^{outrN}(t_{quarter}, S_{RA}, S_{RL}^{in}, S_{RL}^{out}) \\
 & \geq \sum_{S_{RL}^{in}, S_{RL}^{out}} WP_{RA}^{inrN}(t_{quarter}, S_{RA}, S_{RL}^{in}, S_{RL}^{out}) + Q_{RA}^{inrN}(t_{quarter}, S_{RA}, S_{RL}^{in}, S_{RL}^{out}) \\
 & \quad \forall t_{quarter}, t_{hour} = \left\lfloor \frac{t_{quarter}}{4} \right\rfloor, t_{block} = \left\lfloor \frac{t_{quarter}}{16} \right\rfloor \tag{3.40}
 \end{aligned}$$

A full GAMS model with all constraints can be found in Appendix 6.4.1

3.4 Timeline Simulation and Scenario Selection

To develop robust and generally applicable bidding strategies, high-quality data is essential. Inaccurate or poorly constructed datasets inevitably lead to misleading results and suboptimal strategies.

There are various approaches to generating such time series data. We begin with an overview of real-world market data in order to better understand the patterns we aim to replicate or predict, and to identify the key characteristics of the respective electricity markets.

To that end, the market data is first analyzed and visualized using descriptive statistics. Subsequently, different analytical methods are discussed, combined, and applied. This section provides a detailed examination of various techniques for generating representative time series for the various markets.

The data used in this Chapter is from the ENTSOE transparency platform [8] & Regelleistung.net [7].

3.4.1 aFFR - Capacity

In the first panel of the overview [3.1], the real market data from 2023 for the negative capacity market price is displayed. Below that, the corresponding trend and seasonality components are illustrated.

A more detailed examination of the seasonality reveals both a daily and a slight weekly rhythm in the data. Since the dataset refers to 4-hour blocks, every six time lags correspond to a full day. Figure 3.2 clearly illustrates the presence of a daily pattern in the autocorrelation of the data.

Moreover, Figure 3.3 indicates a moderate weekly cycle.

The price development for positive capacity shows a similar behavior to that of the negative capacity prices.

Given the strong autocorrelation in the data, several statistical methods are well-suited for time series analysis and forecasting. In particular, the ARIMA method, which is based on autoregression, proves to be effective for time series with strong autocorrelation. To better

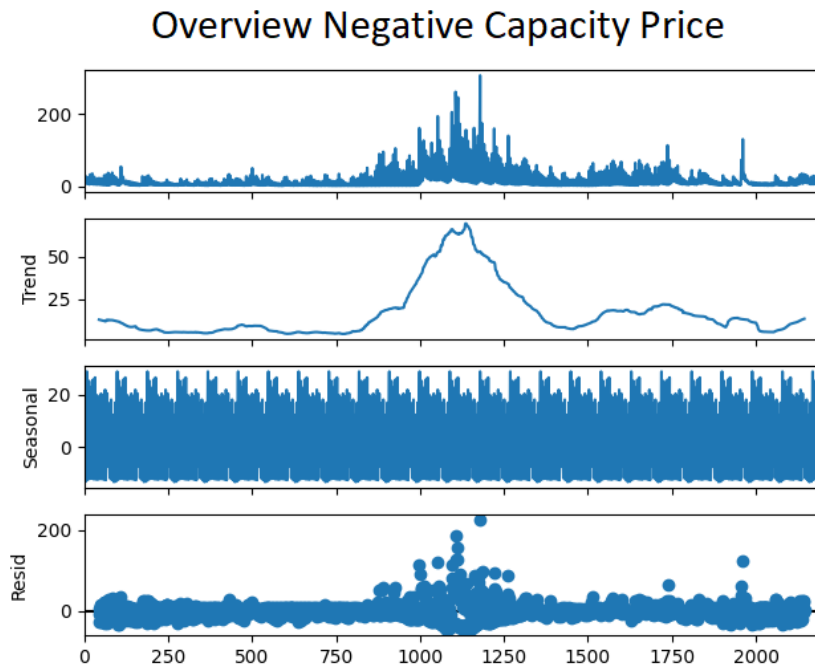


Figure 3.1: Total Average Negative Capacity Price

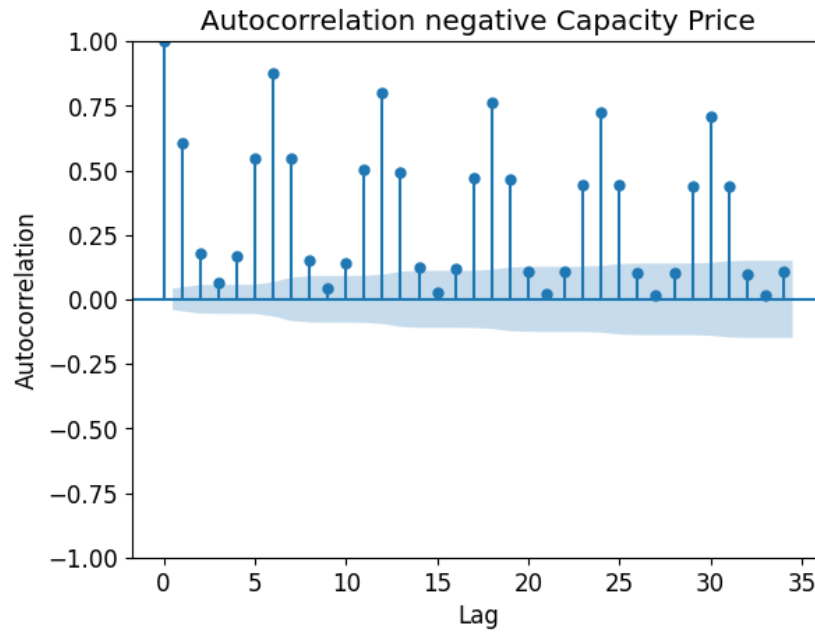


Figure 3.2: Autocorrelation Negative Capacity Price – 5 Days

account for seasonal effects, a seasonal variant of the ARIMA method SARIMA can be applied. But SARIMA struggles with complexity in long time series: computation times increased exponentially, and long-term forecasts tended to be biased towards the most recent trend. Since we expect similar annual patterns in the short term, this bias toward the latest trend is considered unrealistic and undesirable. Moreover, SARIMA is inherently limited to modeling a single seasonal component. To account for multiple seasonalities, extensive manual

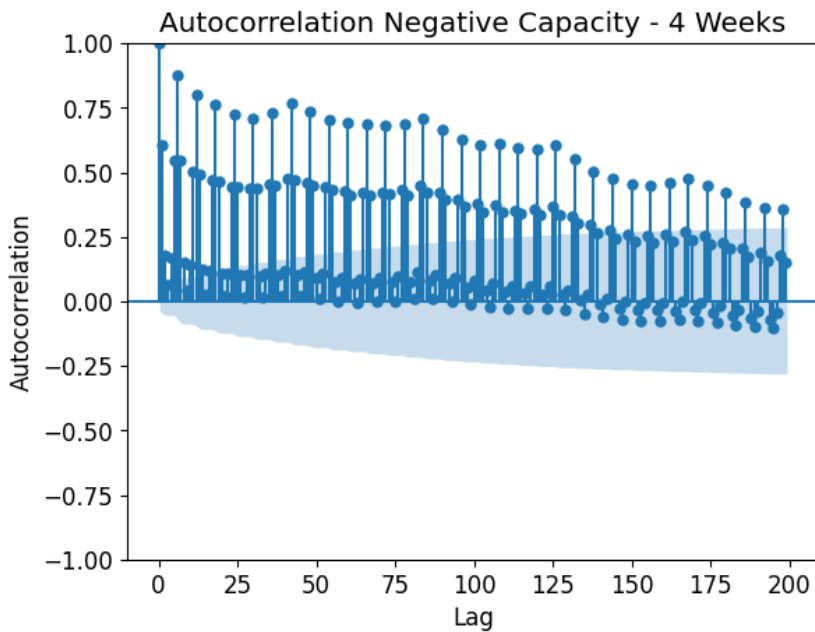


Figure 3.3: Autocorrelation Negative Capacity Price – 4 Weeks

adjustments would be necessary.

A more flexible alternative is the TBATS algorithm, which builds upon similar principles while overcoming these limitations. TBATS stands for Trigonometric seasonality, Box-Cox transformation, ARMA errors, Trend, and Seasonal components. It is implemented in the SKTIME framework and enables efficient forecasting of time series with multiple seasonal patterns [10].

The resulting forecasted time series closely resembles the actual historical time series (Figure 3.4). Note that the timeseries shown here corresponds to the most probable scenario, meaning that 50% of all possible forecast values lie above, and 50% lie below the prediction.

When generating longterm forecast scenarios using the trained predictor, the inherent uncertainty increases with forecasting horizon, resulting in a wider prediction interval (Figure 3.5). While this is methodologically sound and suitable for many use cases, we assume that the mean forecast does not lose accuracy over time and use it as the basis for scenario generation.

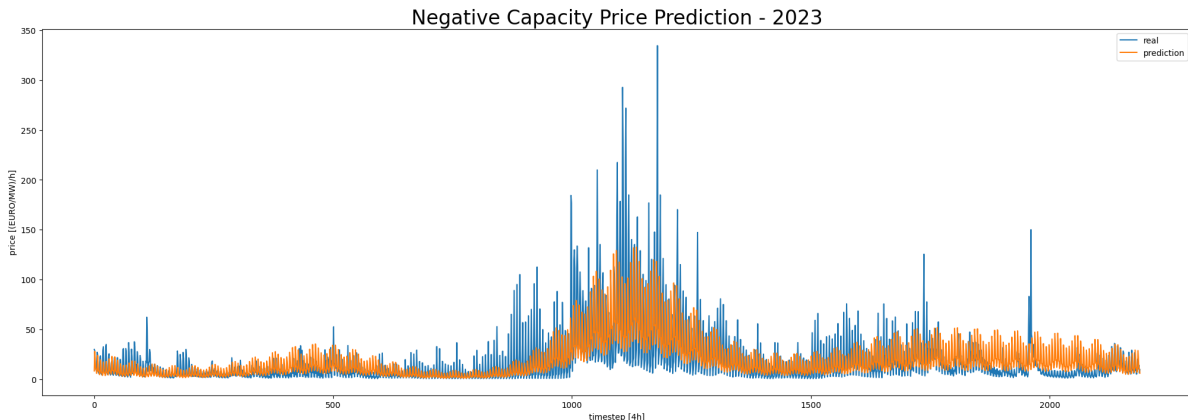


Figure 3.4: Negative Capacity Price Prediction – 2023

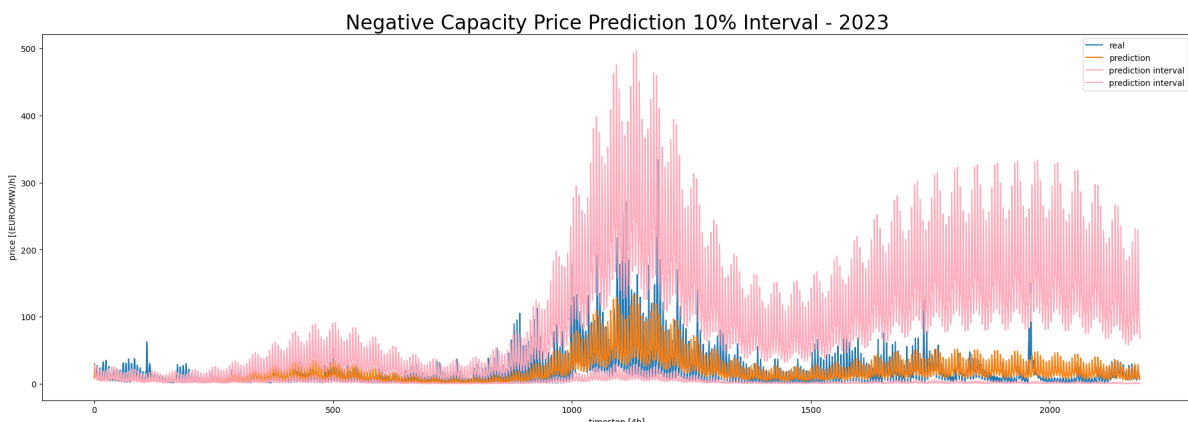


Figure 3.5: Negative Capacity Price Prediction 10%-Interval – 2023

For scenario generation, the median forecast is used and manually scaled upward and downward (e.g., by $\pm 10\%$). These scaled series are then evaluated to determine in how many cases a bidding success would have occurred.

3.4.2 Day Ahead Market

Although the Day-Ahead market prices are variable, they exhibit a daily and weekly rhythm. Over the course of the year, only general trends are observable, as shown in Figure 3.6.

The extraordinary curve movement observed in 2022 (green curve) can be attributed to Russia's war of aggression against Ukraine and the resulting turmoil in the gas market.

Since the Day-Ahead (DA) market operates on a pay-as-cleared mechanism (i.e., all participants receive the price of the highest accepted bid), and we act as a producer of renewable energy with very low operational costs, the model only needs to consider whether we participate in

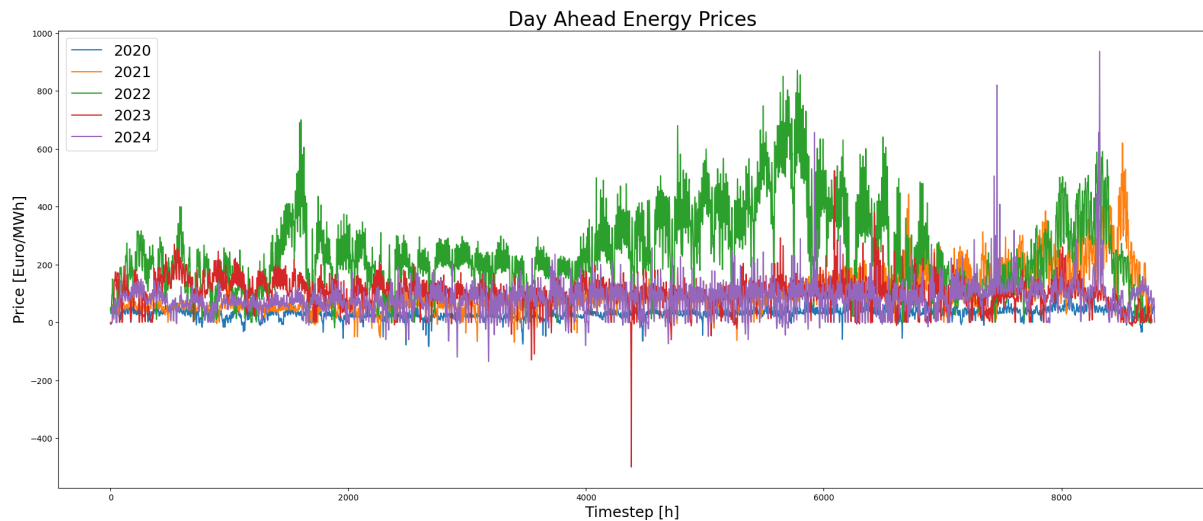


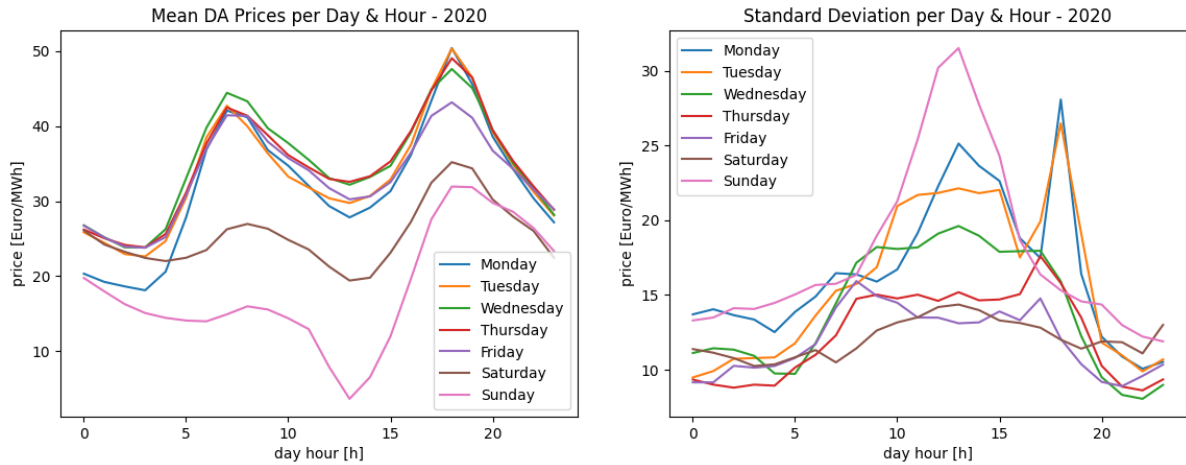
Figure 3.6: Overview DA prices

the market and what the expected clearing price is.

As illustrated in Figures 3.7a to 3.11b, the clearing price exhibits both daily and weekly periodicities. While the overall level of prices may vary, the pattern remains predictable. Due to the market design, it is sufficient for our model to rely on an expected clearing price, as we can realistically submit a zero-price bid and are therefore almost guaranteed to be dispatched.

The expected price used in our model is calculated as the average of the years 2020 through 2024, excluding 2022. This approach preserves the seasonal structure of the data while smoothing out extreme outliers in both directions. Consequently, a reliably expected clearing price can be determined based on time of day, day of the week, and time of year.

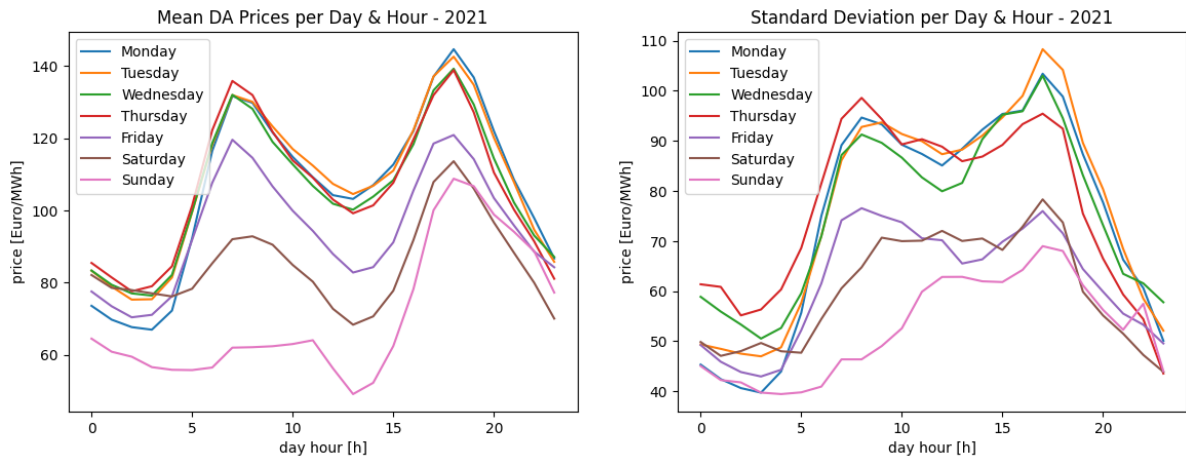
Furthermore, the price level can be adjusted afterward using a simple scaling factor without compromising the inherent structure of the data.



(a) Mean DA-Price

(b) Standard Deviation DA-Price

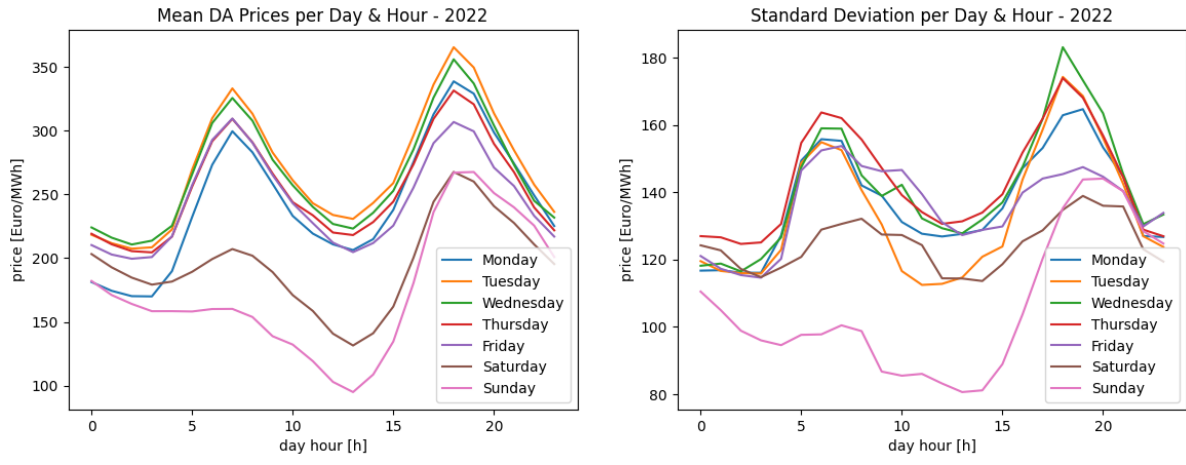
Figure 3.7: Daily and hourly DA-Data - 2020



(a) Mean DA-Price

(b) Standard Deviation DA-Price

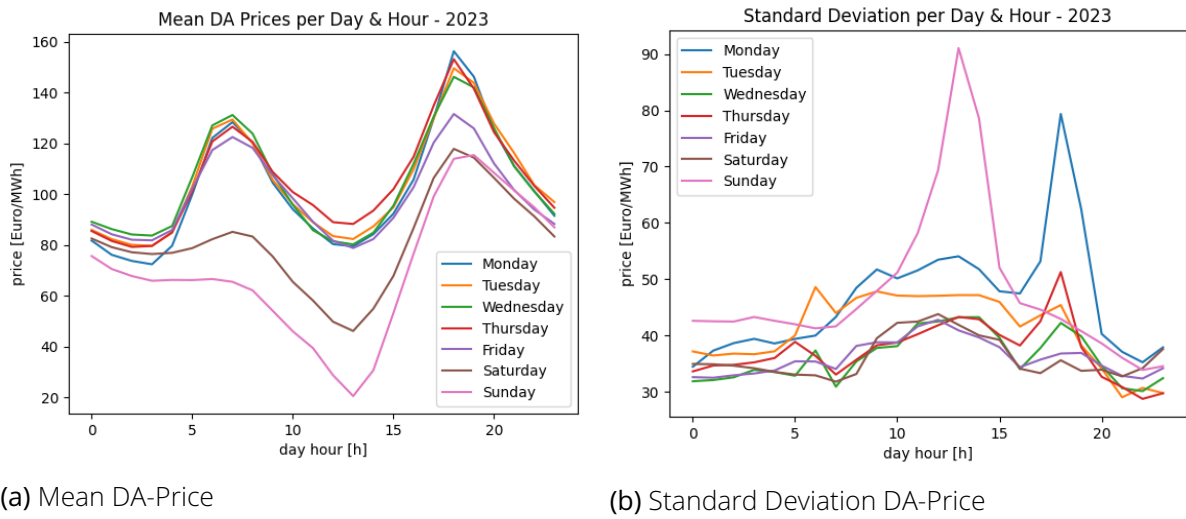
Figure 3.8: Daily and hourly DA-Data - 2021



(a) Mean DA-Price

(b) Standard Deviation DA-Price

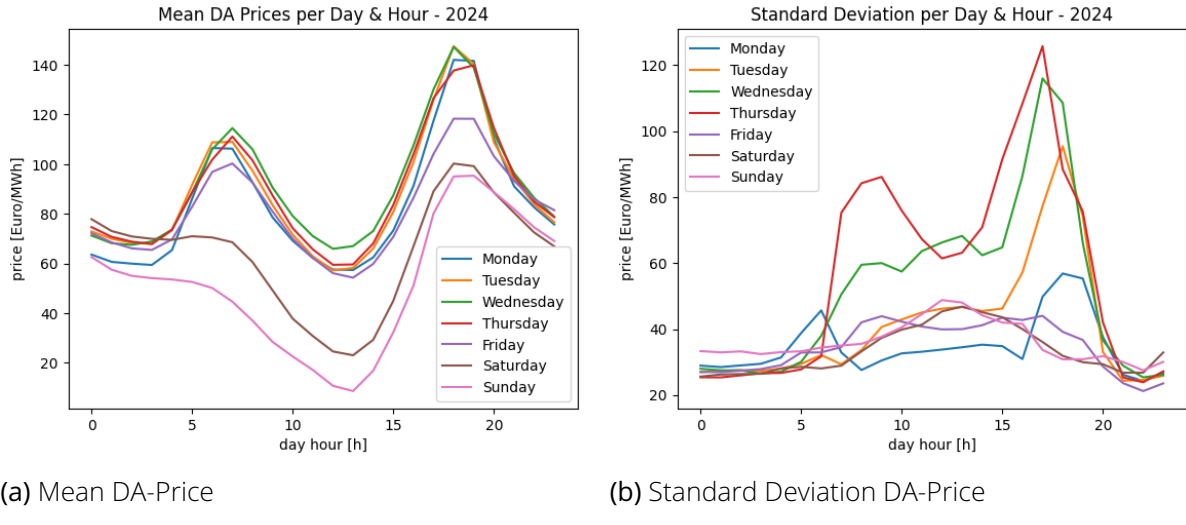
Figure 3.9: Daily and hourly DA-Data - 2022



(a) Mean DA-Price

(b) Standard Deviation DA-Price

Figure 3.10: Daily and hourly DA-Data - 2023



(a) Mean DA-Price

(b) Standard Deviation DA-Price

Figure 3.11: Daily and hourly DA-Data - 2024

Additionally, for the purpose of our simulation, we assume that the simulated renewable energy system represents an onshore wind farm located in Germany. To obtain a wind profile, we divide the total onshore wind power generation by the total installed capacity of these systems [8].

The resulting profile reflects the mean relative wind power output over the entire country. Because wind turbines across Germany are rarely operating simultaneously at zero or full capacity, there are no peaks in this view. In contrast, for an individual wind park, full or zero output can indeed occur. Therefore, in order to give the constraint on maximum grid connection capacity a meaningful interpretation, this average profile needs to be rescaled.

To this end, we treat the national wind production as a proxy for the wind conditions at our specific location. We then apply a scaling transformation that compresses the lower values and expands the higher ones. An additional requirement of the transformation is that the maximum values should be normalized to 1, which corresponds to our wind park operating at full capacity.

This is achieved by first subtracting the mean of the national wind profile, resulting in a series of positive and negative deviations. We then apply a scaling factor to amplify these deviations both upward and downward. Afterward, we add back the original mean to preserve the average and total energy content of the original profile. This transformation yields a new time series whose average matches the original, but whose minimum is 0 and maximum value reaches 1 [3.41].

$$wp_{our} = ((wp_{ger} - wp_{\bar{ger}}) * wsf) + wp_{\bar{ger}} \quad (3.41)$$

The scaling factor is calculated as follows:

$$wsf = \frac{1 - wp_{\bar{ger}}}{\max(wp_{ger}) - wp_{\bar{ger}}} \quad (3.42)$$

3.4.3 aFFR - Energy

The aFFR energy market exhibit a high degree of variability and are extremely difficult to predict statistically. As such, they exhibit only a very weak autocorrelation, as shown in Figure 3.12 (1 lag = 15 min).

No trends are present in the data either. As shown in Figure 3.13, we present 30-day samples from the early, middle, and late parts of the year. In these periods, neither trends nor seasonal developments are observable.

Since no reliable forecasts can be made, real-world data is used for scenario generation. For this purpose, data from the year 2023 was employed [see Table 3.2]. It is observed that solar and onshore wind power plants are particularly subject to volatile production patterns.

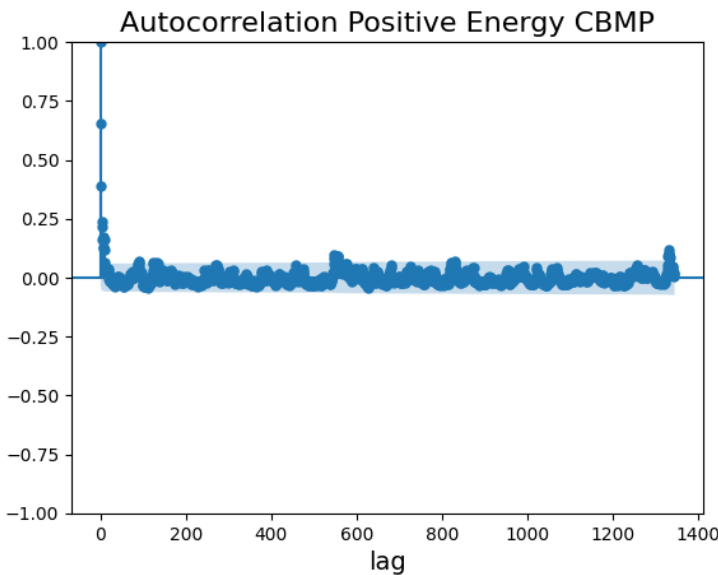


Figure 3.12: Autocorrelation Positive Energy CBMP

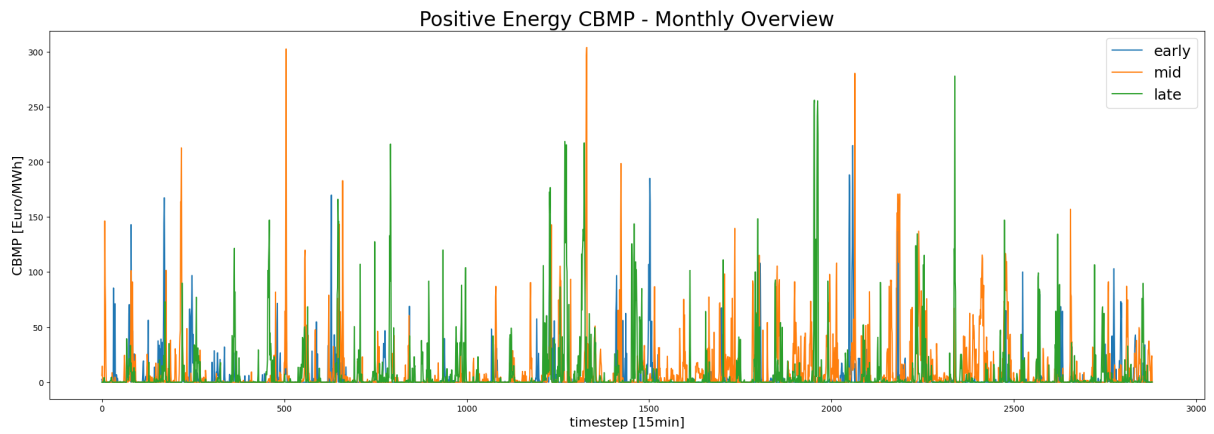


Figure 3.13: Overview Positive Energy CBMP

Subsequently, the total production from solar and onshore wind is calculated for each time point, and divided by the total production of all power plants at the same time. This provides the relative share of these particularly volatile power plants in the overall production. The relative hourly production is then used to determine daily average values.

The hypothesis is that if a prediction error occurs, it has a particularly strong impact when it occurs on days with a high share of volatile production in the overall output.

These relative production data of volatile power plants are then divided into 36 quantiles. The first, median, and last quantiles are used for scenario generation.

For this, the time points of the quantiles, now based on daily data, are extrapolated to a quarter-hourly rhythm, and the corresponding market data from the other markets for the

Source	Standard Deviation
Geothermal	5.956190
Fossil Oil	85.360298
Waste	133.320136
Hydro Water Reservoir	167.126363
Hydro Run-of-river and poundage	310.405850
Biomass	429.594441
Nuclear	1223.169733
Hydro Pumped Storage	1543.402759
Wind Offshore	1833.588012
Fossil Gas	2916.794393
Fossil Hard coal	3364.505964
Fossil Brown coal/Lignite	3799.694920
Solar	9879.907341
Wind Onshore	10506.831136

Table 3.2: Standard deviation per energy generator type

respective time periods are exported. Simultaneously, the matching time periods from the DA and aFFR time series are also exported.

This results in 10 possible scenarios for days with high, medium, and low shares of volatile production. The probabilities are assumed to be evenly distributed, thus each scenario-day has a probability of 10%.

The entire python code and origin data used can be found in Appendix 6.4.2

3.5 Simplifications

In this study, we assume the role of a participant within a bidding consortium. As such, minimum bid requirements can be disregarded, as we assume our consortium partners to be sufficiently large to always meet these minimum thresholds.

To manage the computational effort and reduce the model's complexity, several simplifications have been implemented. These simplifications do not substantially compromise the realism of the model. The following is a structured list of the simplifications employed.

aFFR Capacity/DA Quantile Data

For the time series analyzed, it is important to note that the values are determined based on the preceding day. As a result, the prediction error for the following day has not yet materialized. Consequently, the quantile data for the day ahead aFFR capacity can be averaged over the 10 scenarios days. This approach minimizes unnecessary complexity and allows for more general, strategic conclusions to be drawn regarding bidding behavior in the aFFR capacity/DA market, in relation to potential high, medium, and low prediction errors.

Day Ahead Market

Since the Day-Ahead market operates under a pay-as-cleared structure, our bid influences only the acceptance or rejection of our offer, with no impact on the price paid for the electricity. Given our assumption that we operate a wind farm, we consider operational costs to be negligible, and thus, assume them to be zero. As Day-Ahead prices are non-negative, we can effectively choose whether to submit a bid at a price that will almost certainly be accepted. This results in a simplified optimization for the DA market, represented by $\text{Profit}_{\text{DA}} = Q_{\text{DA}} * p_{\text{DA}}^{\text{exp}}$. We further assume our specific renewable production forecast as perfect.

aFFR Energy Market

As the aFFR Energy Market market also follows a pay-as-cleared principle, our bid influences only whether we are called upon to deliver, with no impact on the price paid for the electricity. Assuming the role of a battery storage operator with near-zero operational costs, these are

considered negligible. Thus, we can submit a bid below the expected RA market price to ensure that our offer is likely to be called. The reverse is also true.

When an aFFR capacity bid is accepted, we are obligated to submit a corresponding aFFR energy bid. This creates a constraint that limits the minimum bid quantity in the aFFR energy market based on the accepted aFFR capacity bid quantity. However, integrating the introduced case would lead to an increase in computational complexity due to the need for extra variables and additional dimensions. In practice, this regulatory constraint can be bypassed by setting a sufficiently high working price, ensuring that our bid is not called upon. Therefore, this constraint was not explicitly incorporated into the model. But, we incorporated a constraint that links the minimum and maximum *BatStat* to the accepted aFFR energy bids. This ensures that, at all times during the relevant aFFR block, sufficient storage capacity is available to fulfill any potential requests. This approach avoids the computationally intensive direct linkage between the aFFR capacity and aFFR energy markets while still accurately reflecting the underlying mechanisms.

Battery Storage Status

The battery storage status is recalculated at 15-minute intervals. The battery status from the previous time window is updated by adding all inflows and subtracting all outflows. Given the uncertainty of these inflows and outflows, multiple possible battery states would arise at the end of each calculation window, based on the possible preceding states. Since we calculate the battery status over 96 consecutive time periods, the computational complexity would increase exponentially due to the number of possible outcomes over these 96 periods. Even with only two considered scenario outputs, this results in

$$2^{96} = 79228162514264337593543950336$$

possible battery storage states at the end of the day. Considering that planning always takes place for the following day, one would need to account for

$$2^{182} = 6.13 \times 10^{54}$$

possible battery storage states before achieving planning certainty again. Since a full enumeration of all possible future system states quickly becomes computationally infeasible, it is

necessary to either assume perfect foresight and calculate a single, most probable trajectory for the battery storage system, or to approximate certain processes along the time series. Therefore, we approximate the battery storage calculation by determining an expected battery status at time $t_{quarter}$ and using this expected value for subsequent calculations. Inflows and outflows are weighted by their respective probabilities, allowing for an approximation of the correct battery status over the entire period.

This method inherently flattens the battery loading status curve, depending on the assumed probability distributions. For example in reality, consecutive 10% fluctuations may occur, leading to a more pronounced shift in the battery status than the model predicts. To ensure that the storage capacity meets the required levels, the actual capacity have to be recalculated by considering unweighted quantity bids and determining the maximum fluctuation. This value corresponds to the actual required storage capacity. As the storage/bid ratio increases, the impact of this adjustment becomes negligible, as the likelihood of consecutive unlikely events diminishes over time.

4 Results

To properly contextualize the results, we begin by briefly presenting the initial data.

The relative production quantiles, which were used to segment the other time series, are illustrated as follows:

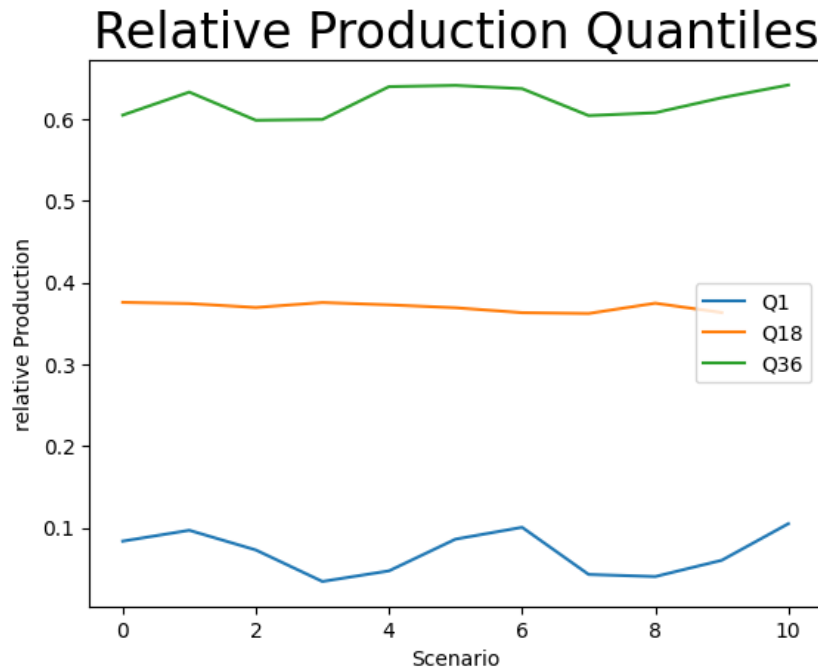


Figure 4.1: Relative Production Quantiles

Based on these, the resulting time series for activated balancing energy and their corresponding prices are shown below: The corresponding data for the aFFR market is presented in the Appendix 6.2. The data indicate that, with increasing market penetration of volatile energy sources, the volume of activated negative balancing energy increases, whereas the demand for positive balancing energy tends to decrease. A similar pattern emerges in the marginal prices for activated balancing energy. While the prices for negative balancing energy rise with a higher share of volatile producers, the prices for positive balancing energy decline. Notably, there are significant outliers in the time series of marginal prices for positive balancing energy, especially in scenarios with medium and low market penetration of volatile producers.

The median balancing capacity prices peak for both negative and positive in the medium volatility scenario. In the first quantile's data, the prices for negative capacity are comparable to those in the 36th quantile. For positive balancing energy, however, the 36th quantile diverges

significantly from the 1st quantile, especially during the later hours of the day.

Based on these time series, the model produced the following results:

The bidding strategy for capacity market prices consistently remains just below the expected marginal price across all scenarios. The optimization selects a bid price equal to 90% of the expected marginal market price.

It can be observed that the provision of negative balancing energy occurs earlier in the low and medium scenarios when both balancing power bids are accepted [Figure 4.2, 4.4]. This temporal shift is not observed in scenarios with high volatility energy production penetration [Figure 4.6].

While the bidding quantities for positive balancing energy remain largely consistent across low and medium volatility scenarios, regardless of capacity market acceptance, more pronounced differences appear under high-volatility conditions. In these scenarios, earlier energy provision also results from tighter restrictions due to capacity market results.

To aid in interpretation, we define the following restriction categories:

1. Restricted: B → RL accepted for both input and output (blue)
2. Restricted: O → RL accepted for output, declined for input (orange)
3. Restricted: I → RL accepted for input, declined for output (green)
4. Restricted: N → RL declined for both input and output (red)

The results indicate a relatively consistent bidding behavior in the capacity market across all scenarios.

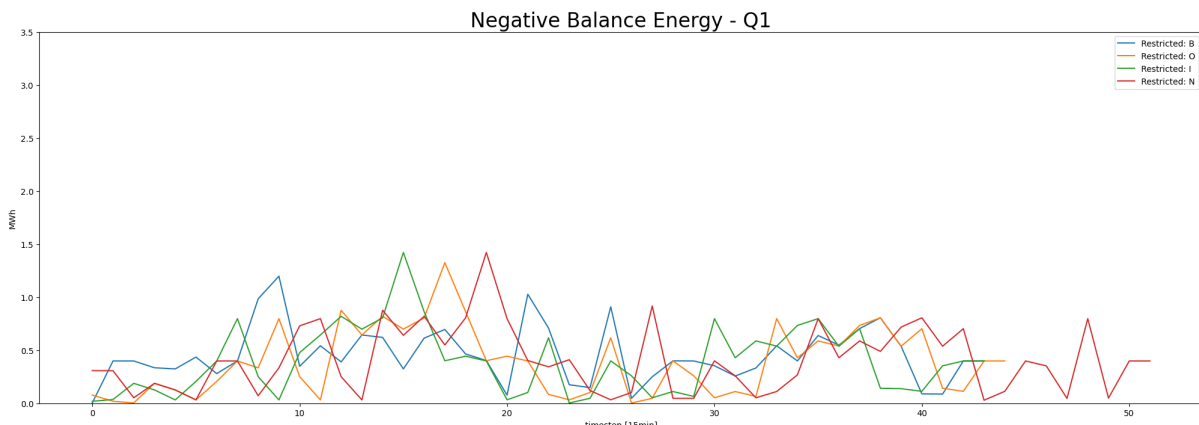


Figure 4.2: Negative Balance Energy - Q1

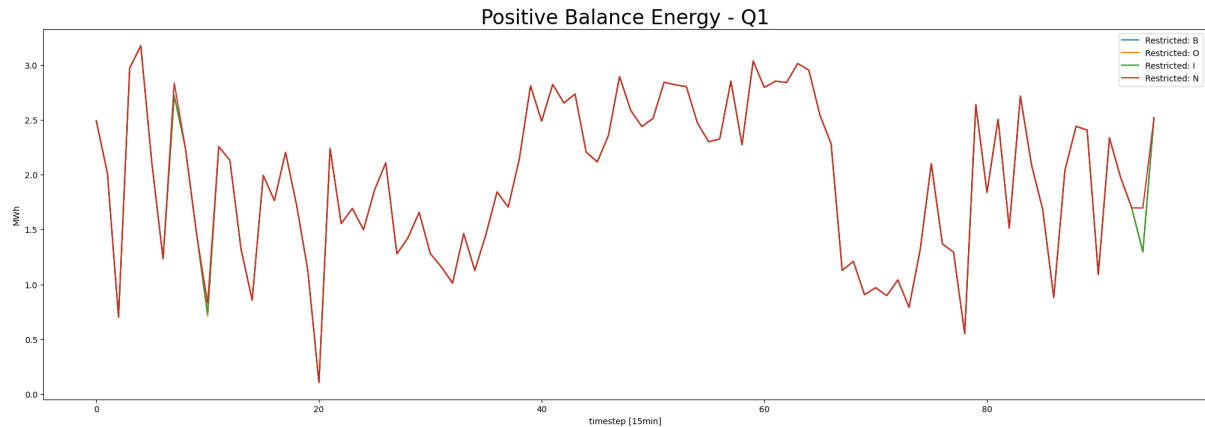


Figure 4.3: Positive Balance Energy - Q1

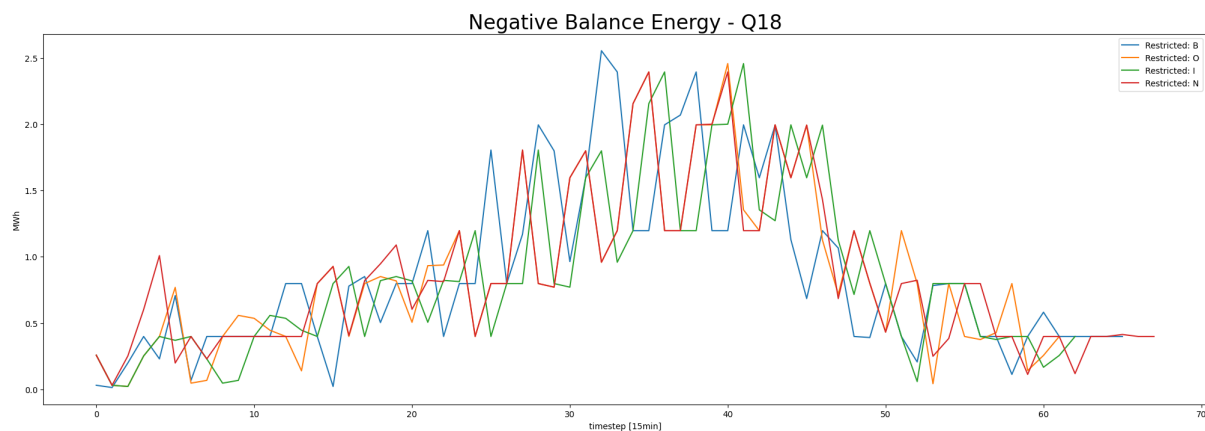


Figure 4.4: Negative Balance Energy - Q18

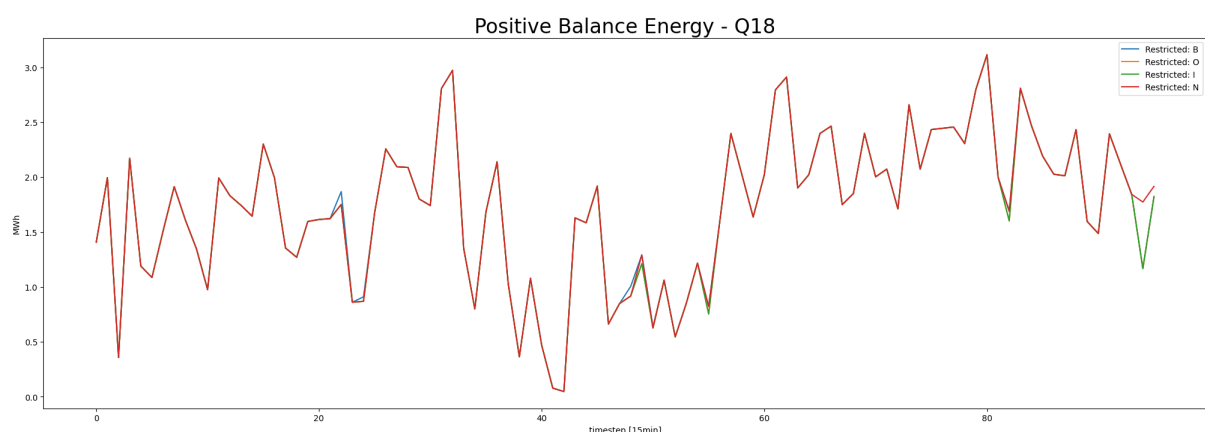


Figure 4.5: Positive Balance Energy - Q18

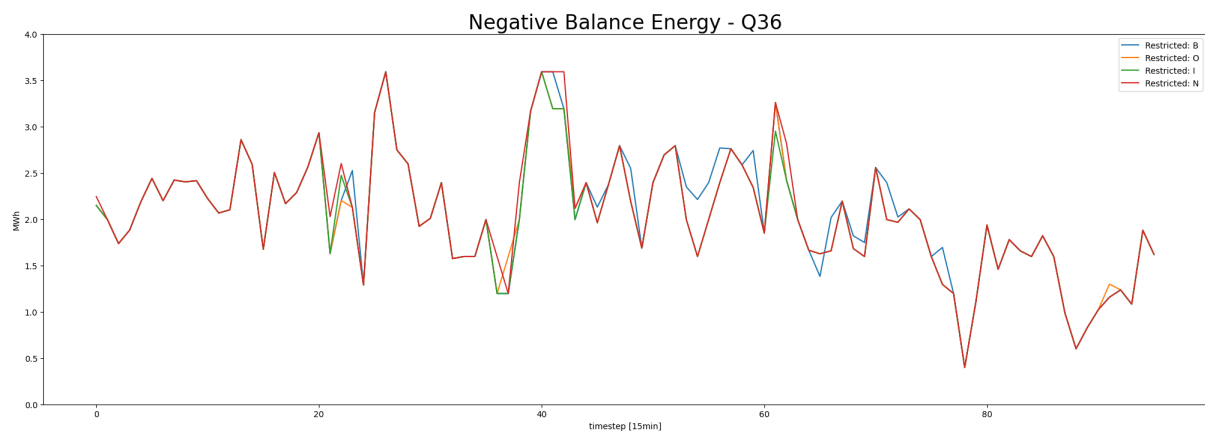


Figure 4.6: Negative Balance Energy - Q36

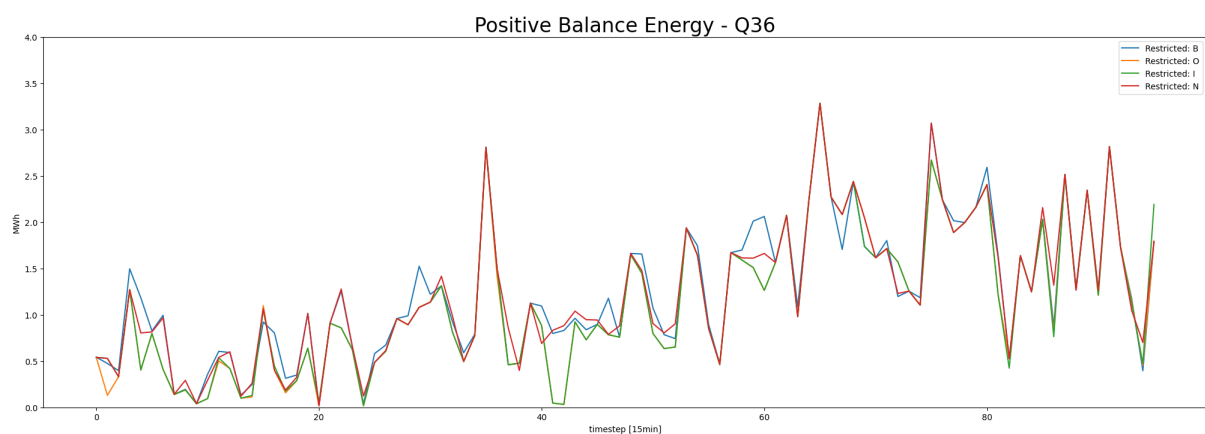


Figure 4.7: Positive Balance Energy - Q36

5 Conclusion

The analyses presented in this work clearly demonstrate that increasing market penetration by volatile energy producers has significant effects on both the utilization and pricing of balancing markets. In particular, it is observed that with a growing share of volatile generation, the volume of activated negative balancing energy increases, while demand for positive balancing energy decreases. This pattern is also reflected in the marginal prices: while the prices for negative balancing energy tend to rise with increasing generation volatility, the prices for positive balancing energy show a declining trend.

Notably, strong price outliers can be observed for positive balancing energy in scenarios with low or medium market penetration by volatile producers. These anomalies appear to be driven by unexpectedly high demand peaks in scenarios where market participants did not anticipate major fluctuations. This suggests that the expectations and preparedness of market participants play a crucial role in maintaining price stability under conditions of variable renewable energy feed-in.

The analyzed aFFR capacity prices reveal a nuanced picture: in median quantile scenarios, values peak for both positive and negative balancing capacity, indicating decreasing supply in this setting. This may be due to the fact that, in the respective aFFR energy scenarios with attractive price levels, the corresponding capacity market is perceived as a side benefit. This behavior leads to a supply increase that exceeds the rise in demand, resulting in falling capacity prices. In scenarios with low aFFR prices, the underlying cause appears to be a generally low level of demand. However, a conclusive analysis requires further investigation.

Across all scenarios, the bidding strategies for the balancing capacity market prices are positioned just below the expected marginal prices.

In scenarios with low to medium levels of volatile production penetration, the introduction of constraints through the aFFR capacity market leads to a shift towards earlier provisioning in the negative balancing energy market. This is reflected in a more regular schedule of negative balancing energy delivery. In contrast, in high volatility scenarios with elevated prices, a strategy focused on capitalizing on price peaks becomes evident. In such cases, providers may choose to forgo profits in the capacity market in order to place their bids more flexibly in the energy market. This strategy aims to take better advantage of price peaks in the aFFR

energy market.

It is also worth noting that, while the model accounts for different possible aFFR energy market scenarios, it assumes perfect foresight within each individual daily scenario. As a result, the revenue potential from the aFFR energy market is likely overestimated. Moreover, the model heavily exploits price peaks, which may not be fully realizable in practice. Whether such behavior can be implemented in reality depends largely on the quality of intraday forecasts and requires further investigation.

An alternative modeling approach would be to refrain from using precise price data for the aFFR energy market and instead attempt to represent general market cycles. Under the hypothesis that the transmission system operator continuously strives to balance the grid, it can be postulated that any imbalance will eventually be corrected. Prolonged imbalances are assumed to be relatively unlikely. Based on this assumption, certain recurring patterns could be forecasted within a 4-hour window, characterized by a defined expected value. Appendix 6.4.3 presents a preliminary model approach for this idea. However, both the scientific validation of the underlying hypothesis and the development of a suitable aFFR prediction cycle algorithm remain subjects for further research.

For positive balancing energy, the analysis reveals that bidding volumes in low and medium volatility scenarios differ only marginally depending the aFFR capacity market. Pronounced differences emerge only in high-volatility scenarios. Again, the data show that the more restrictive the capacity market constraints, the earlier the provision of balancing energy occurs.

Since the model considered only a single day, it is possible that the positive effects of battery charging via the wind farm have not yet been fully realized. Additional benefits may arise from the battery serving as a backup in cases of forecasting errors in renewable energy generation, thereby helping to avoid potential costs. To better assess both effects, further research is required.

In summary, basic strategic guidelines can be derived from our model. However, further research is required to develop precise decision criteria and the resulting actionable strategies.

6 Appendix

6.1 Further Model Constraints

$$\sum_{S_{DA}, S_{RL}^{in}, S_{RL}^{out}} Q_{DA}^{rB}(t_{hour}, S_{RL}^{in}, S_{RL}^{out}) \leq parkCap * parkProfile(t_{hour}) - \sum_{S_{DA}, S_{RL}^{in}, S_{RL}^{out}} Q_{reload}^{rB}(t_{hour}, S_{RL}^{in}, S_{RL}^{out}) \quad (6.1)$$

$$\sum_{S_{DA}, S_{RL}^{in}, S_{RL}^{out}} Q_{DA}^{rl}(t_{hour}, S_{RL}^{in}, S_{RL}^{out}) \leq parkCap * parkProfile(t_{hour}) - \sum_{S_{DA}, S_{RL}^{in}, S_{RL}^{out}} Q_{reload}^{rl}(t_{hour}, S_{RL}^{in}, S_{RL}^{out}) \quad (6.2)$$

$$\sum_{S_{DA}, S_{RL}^{in}, S_{RL}^{out}} Q_{DA}^{rO}(t_{hour}, S_{RL}^{in}, S_{RL}^{out}) \leq parkCap * parkProfile(t_{hour}) - \sum_{S_{DA}, S_{RL}^{in}, S_{RL}^{out}} Q_{reload}^{rO}(t_{hour}, S_{RL}^{in}, S_{RL}^{out}) \quad (6.3)$$

$$\sum_{S_{DA}, S_{RL}^{in}, S_{RL}^{out}} Q_{DA}^{rN}(t_{hour}, S_{RL}^{in}, S_{RL}^{out}) \leq parkCap * parkProfile(t_{hour}) - \sum_{S_{DA}, S_{RL}^{in}, S_{RL}^{out}} Q_{reload}^{rN}(t_{hour}, S_{RL}^{in}, S_{RL}^{out}) \quad (6.4)$$

6.2 Quantile aFFR Market Data

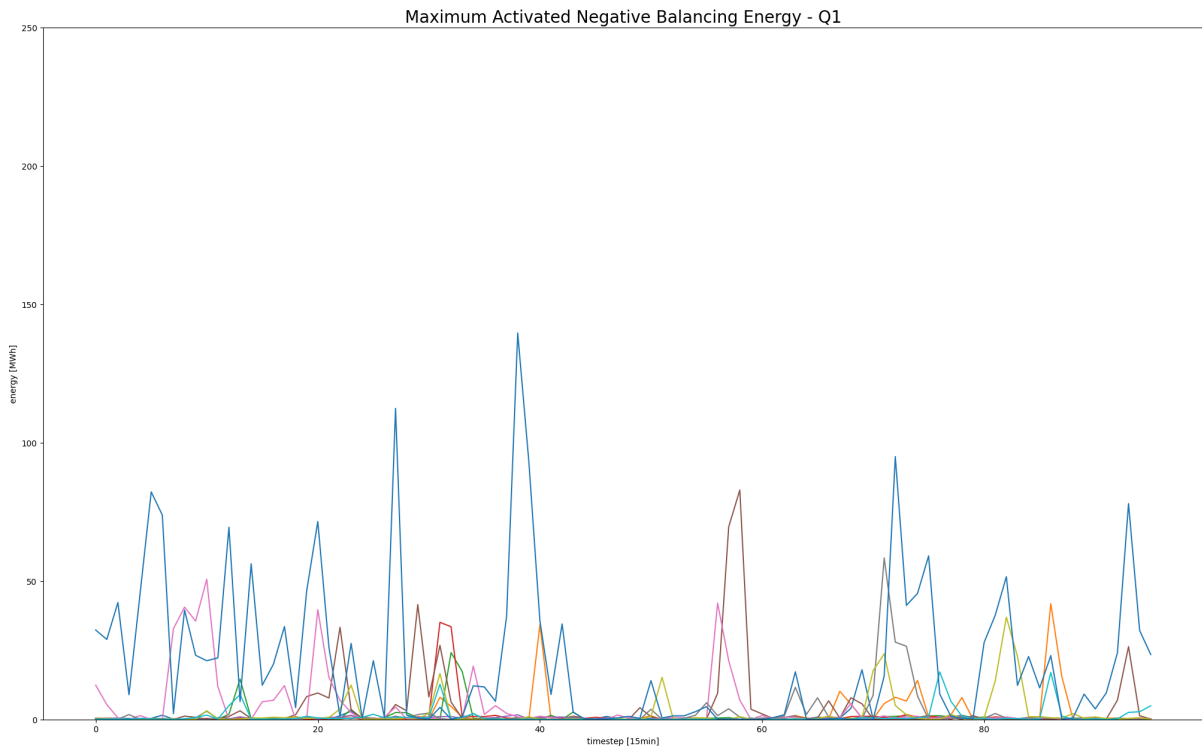


Figure A.1: Activated Negative Energy Q1

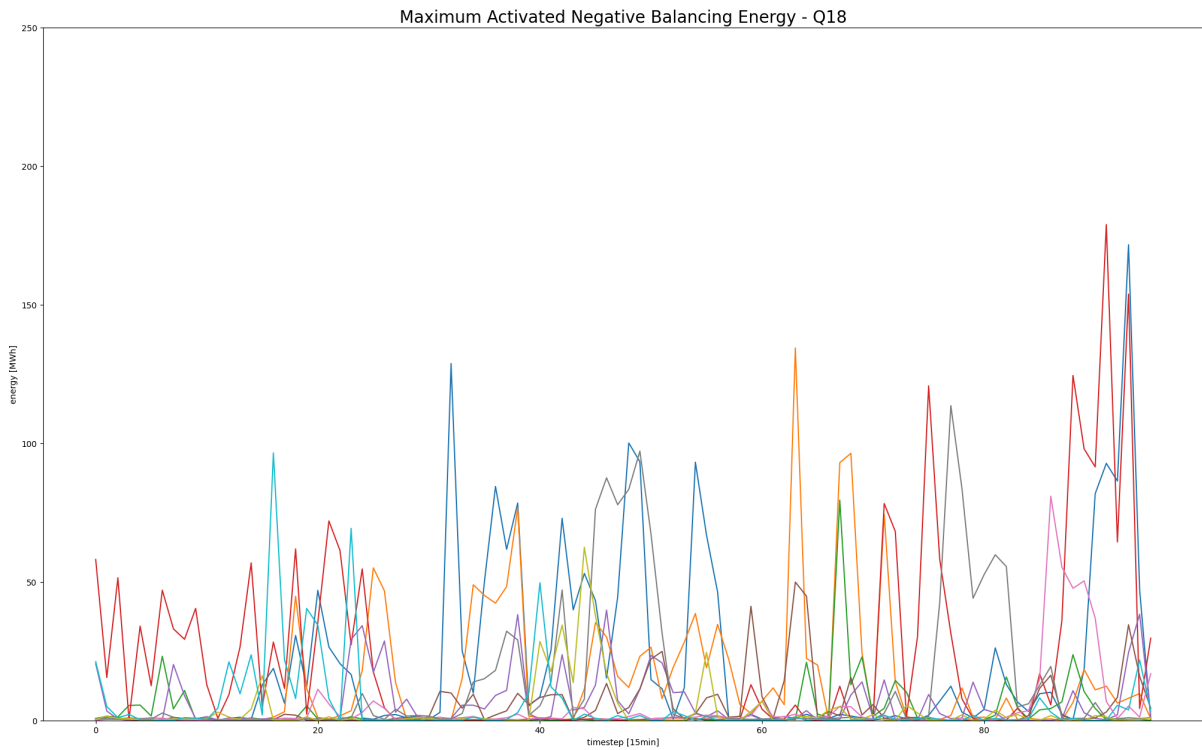


Figure A.2: Activated Negative Energy Q18

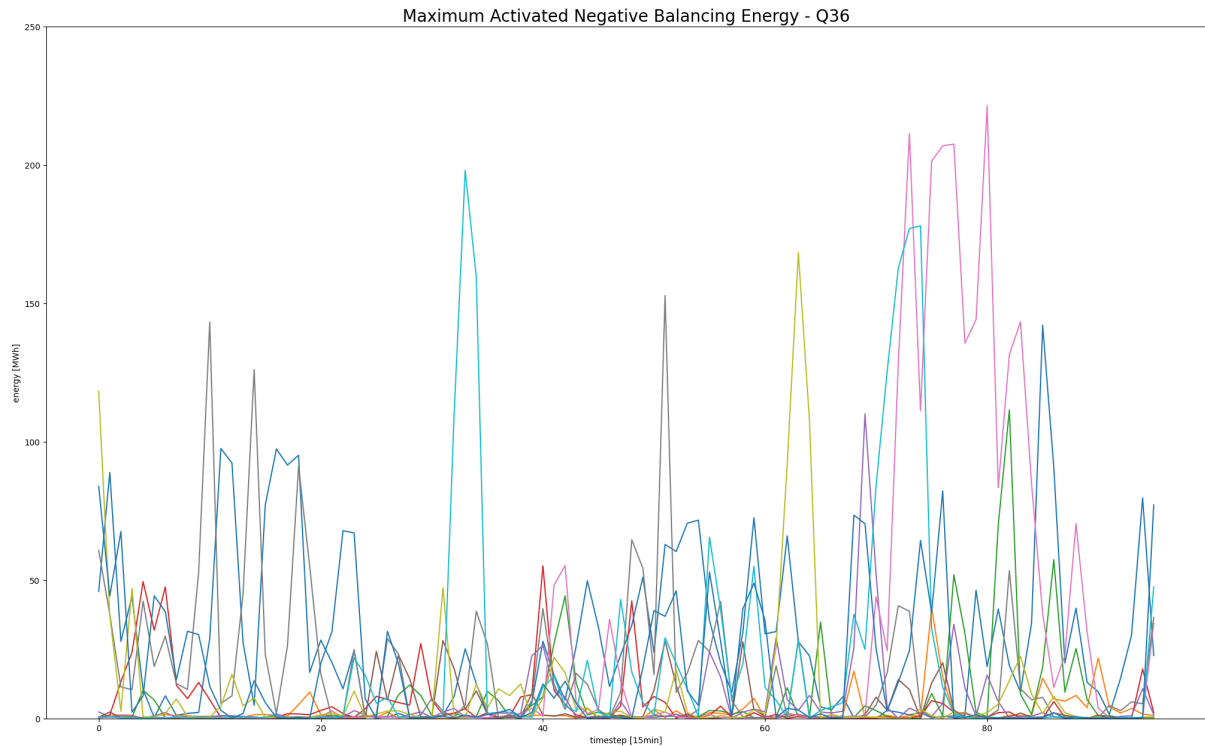


Figure A.3: Activated Negative Energy Q36

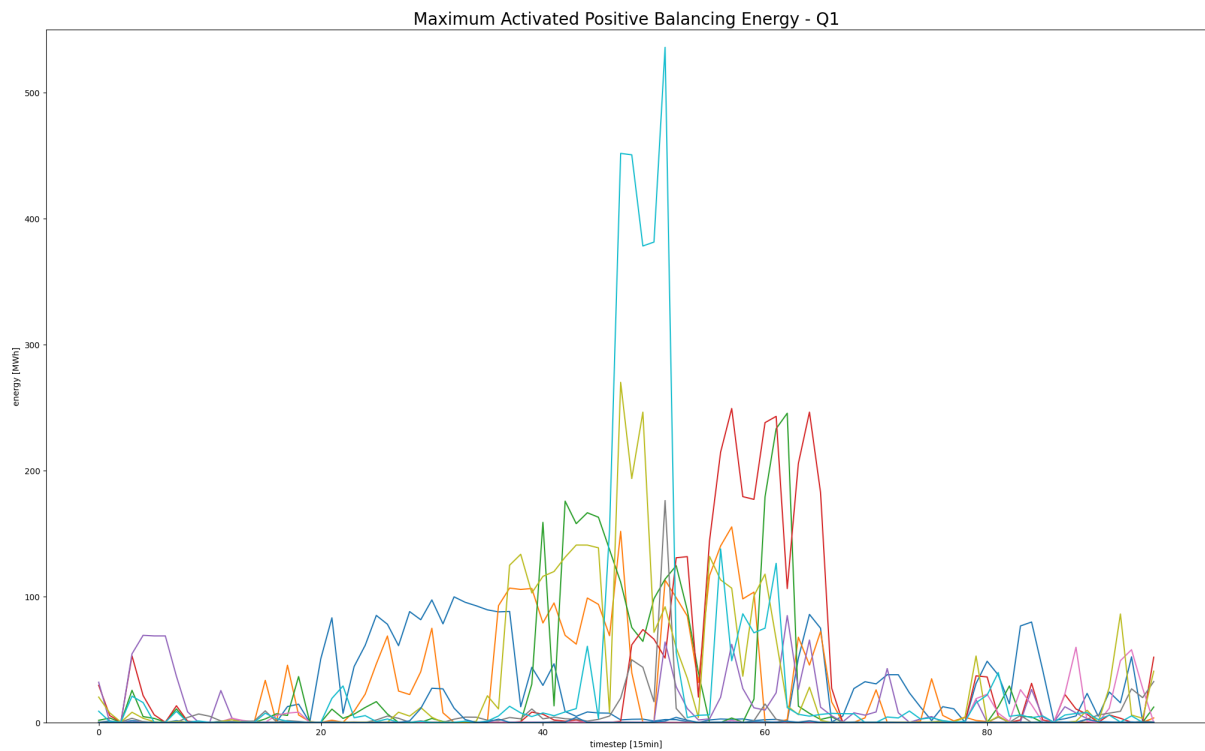


Figure A.4: Activated Positive Energy Q1

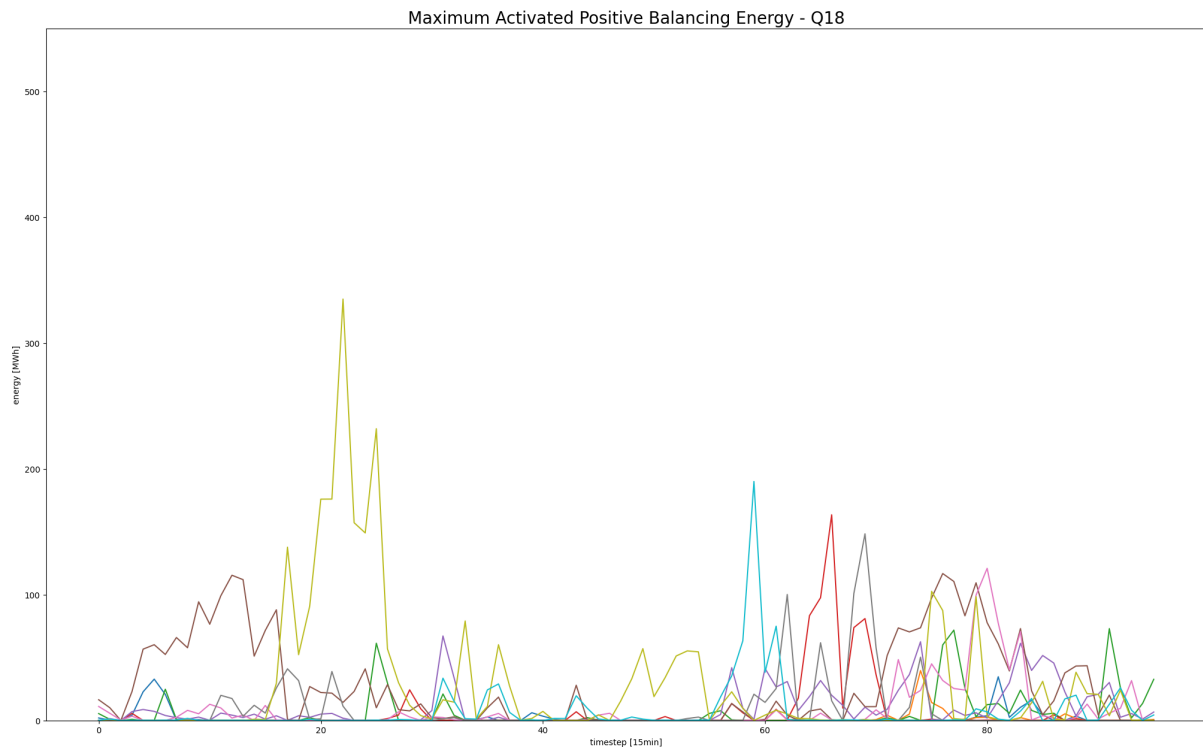


Figure A.5: Activated Positive Energy Q18

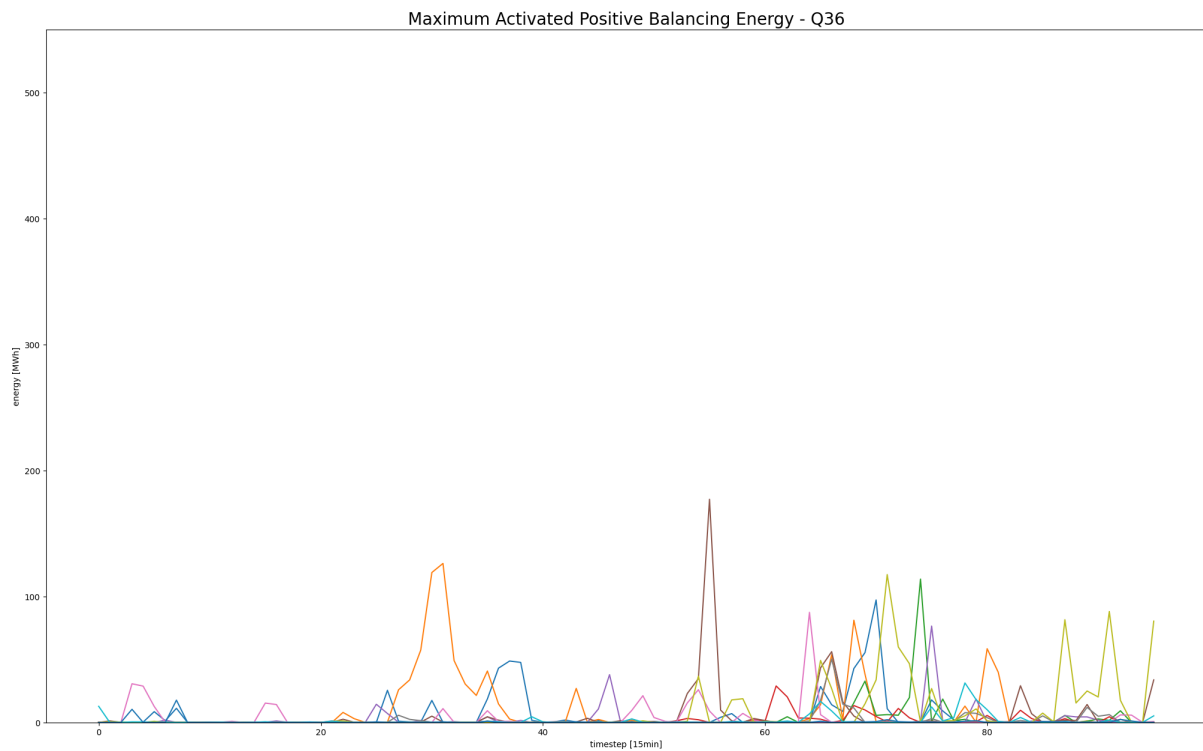


Figure A.6: Activated Positive Energy Q36

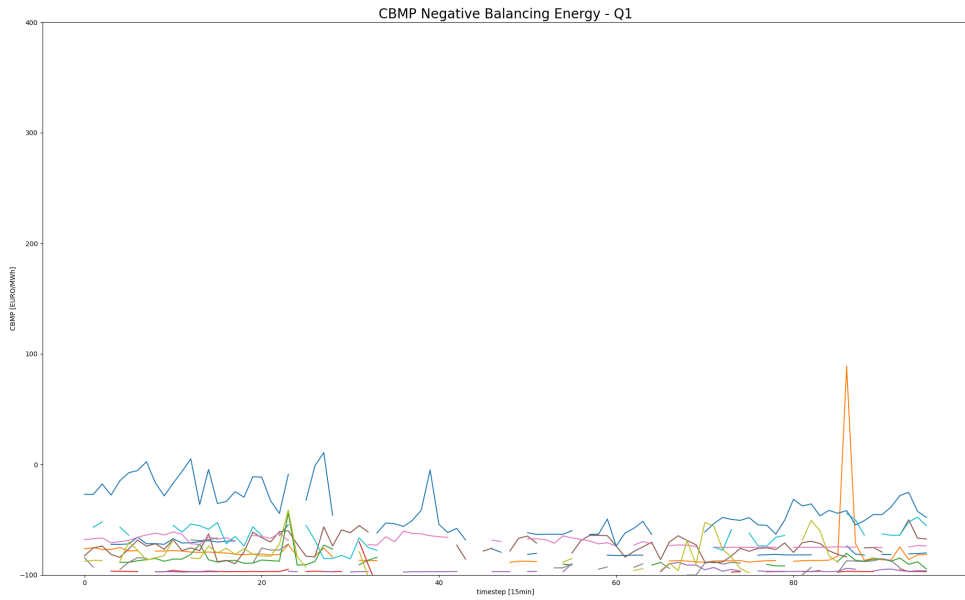


Figure A.7: CBMP Negative Energy Q1

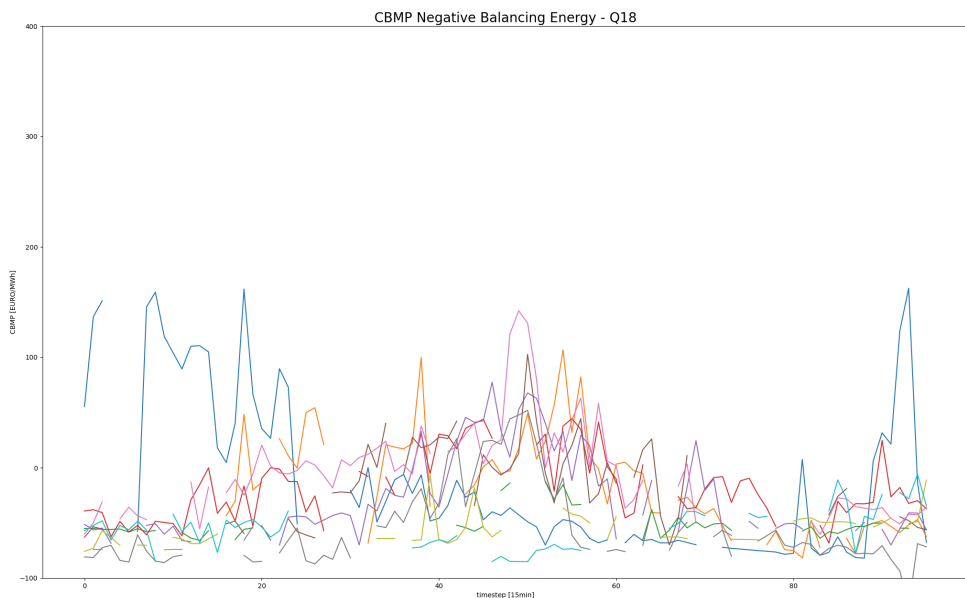


Figure A.8: CBMP Negative Energy Q18

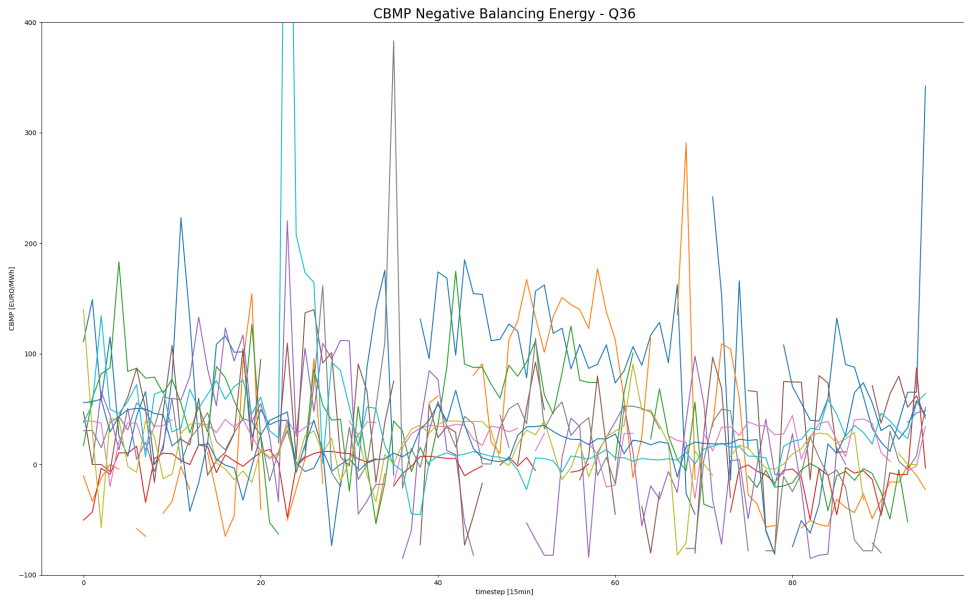


Figure A.9: CBMP Negative Energy Q36

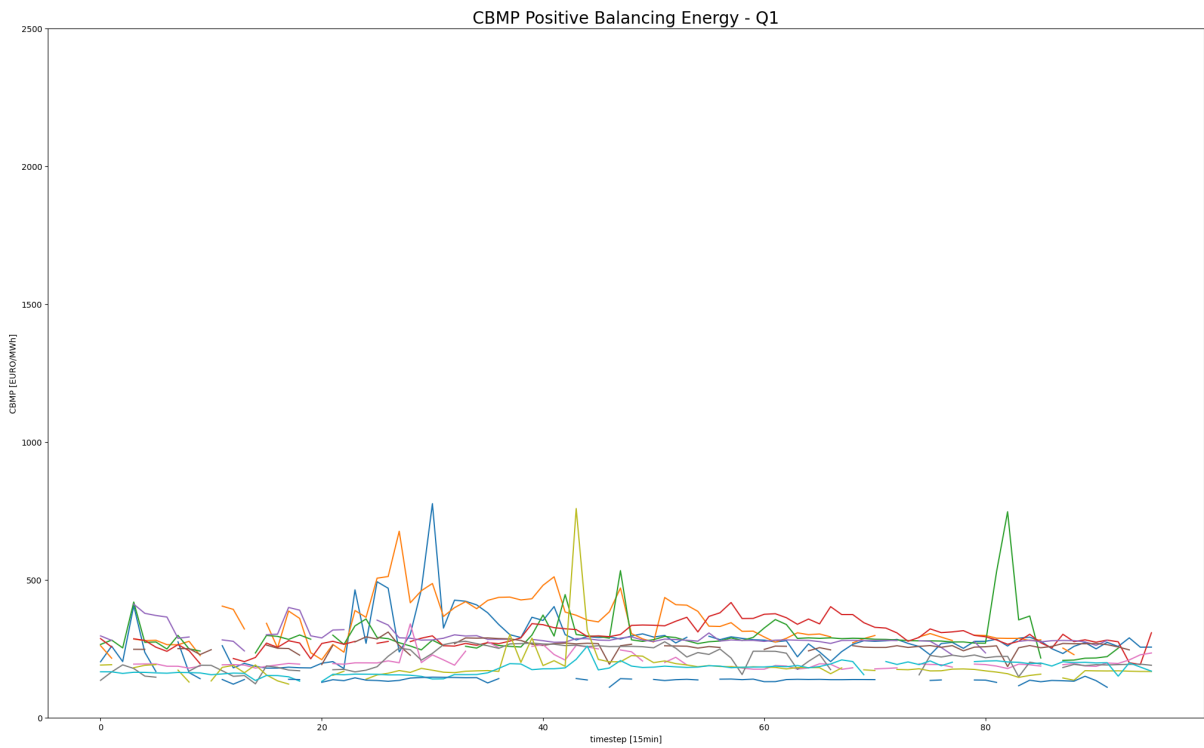


Figure A.10: CBMP Positive Energy Q1

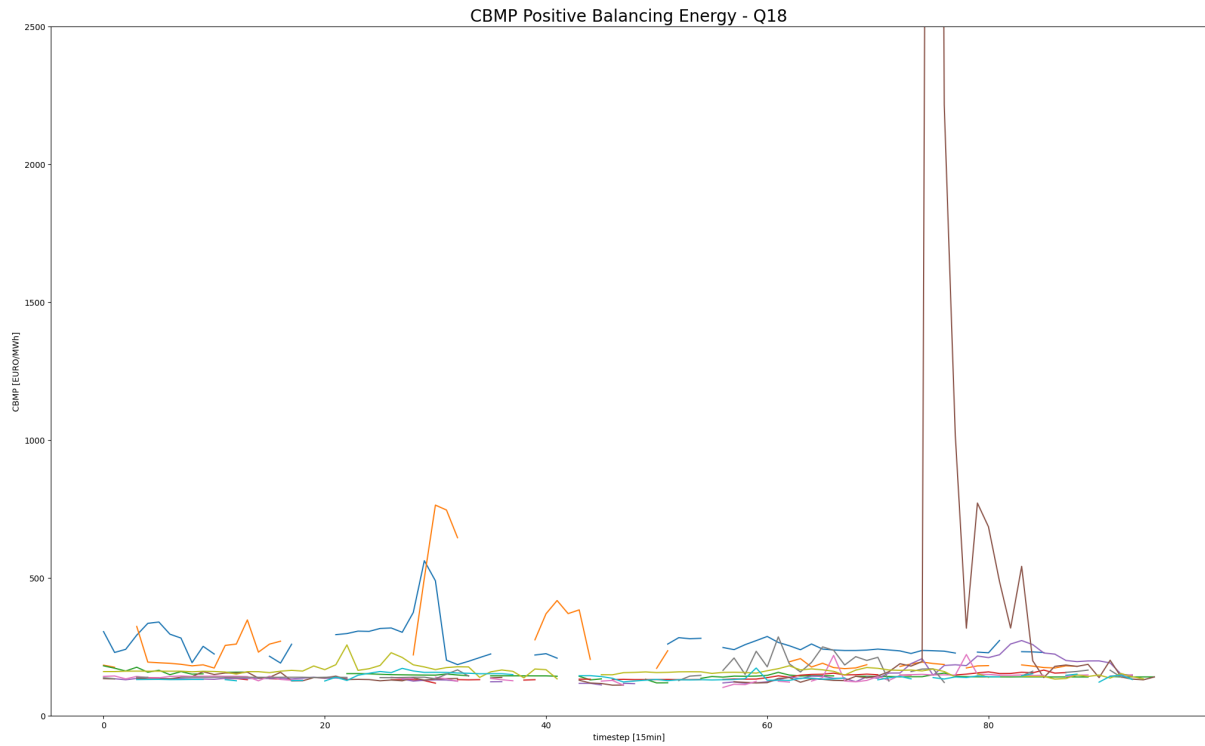


Figure A.11: CBMP Positive Energy Q18

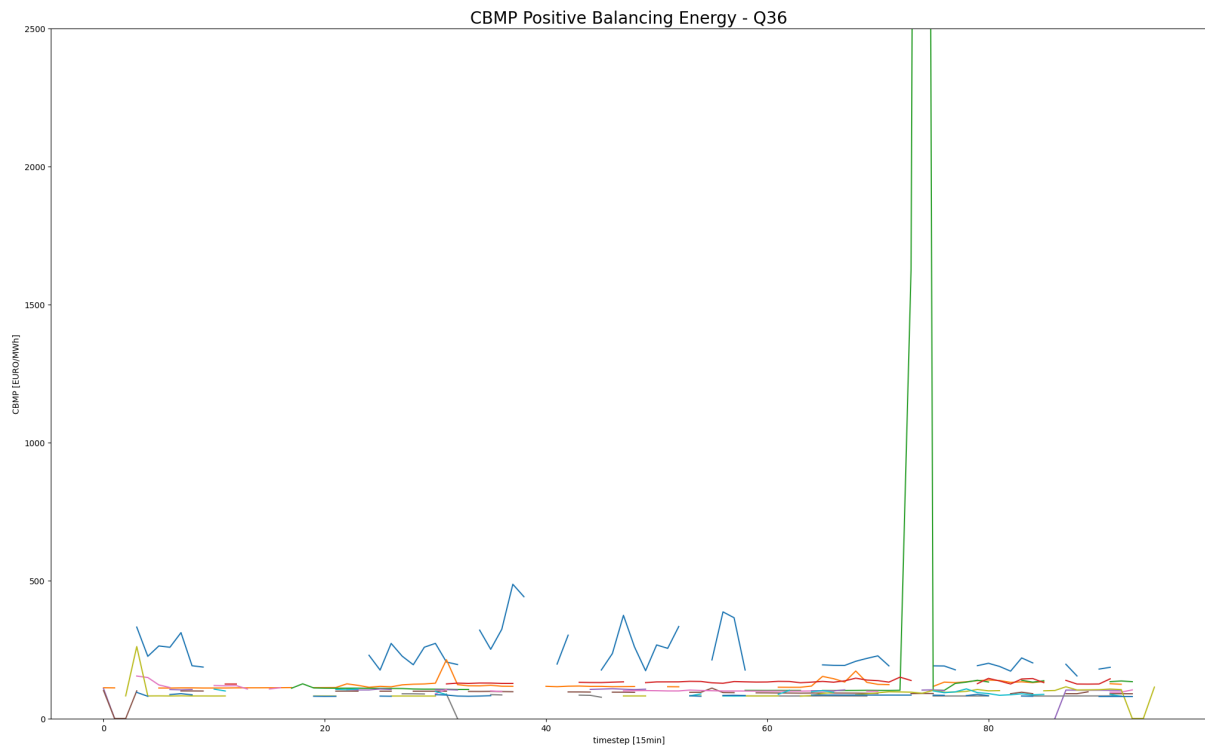


Figure A.12: CBMP Positive Energy Q36

DA

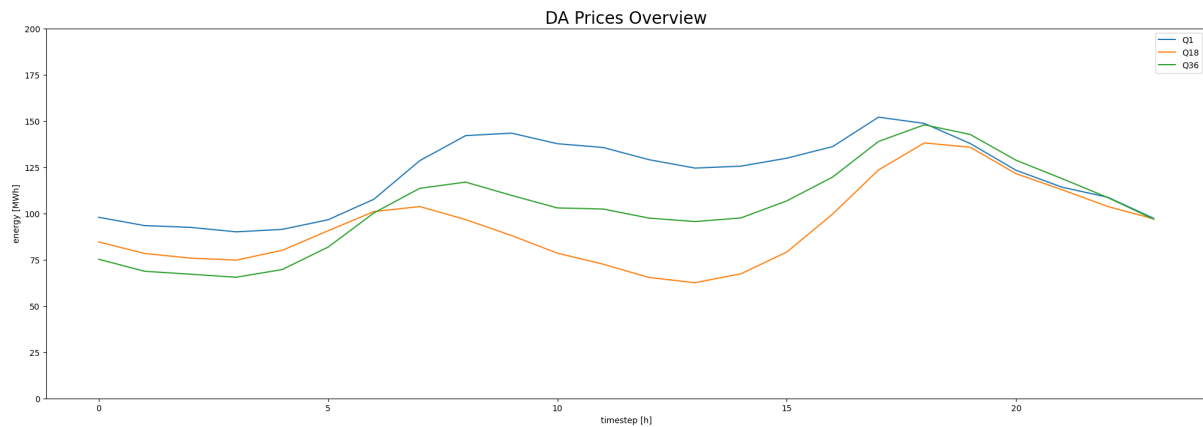


Figure A.13: DA Prices

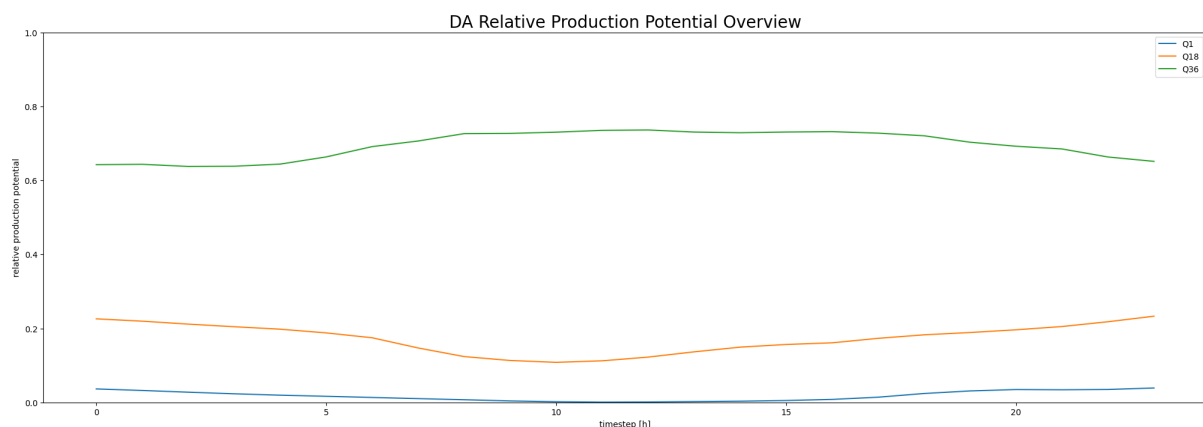


Figure A.14: DA Production

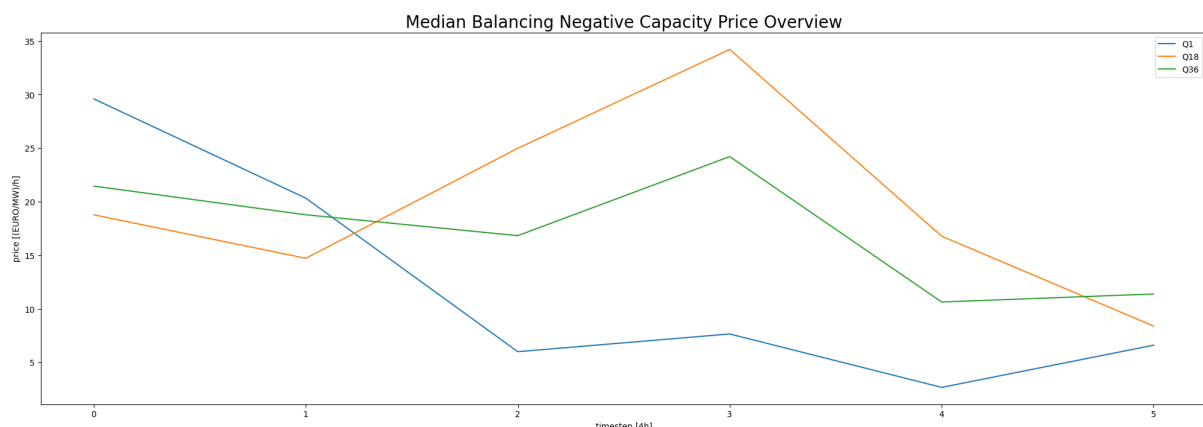


Figure A.15: RL Negative Prices

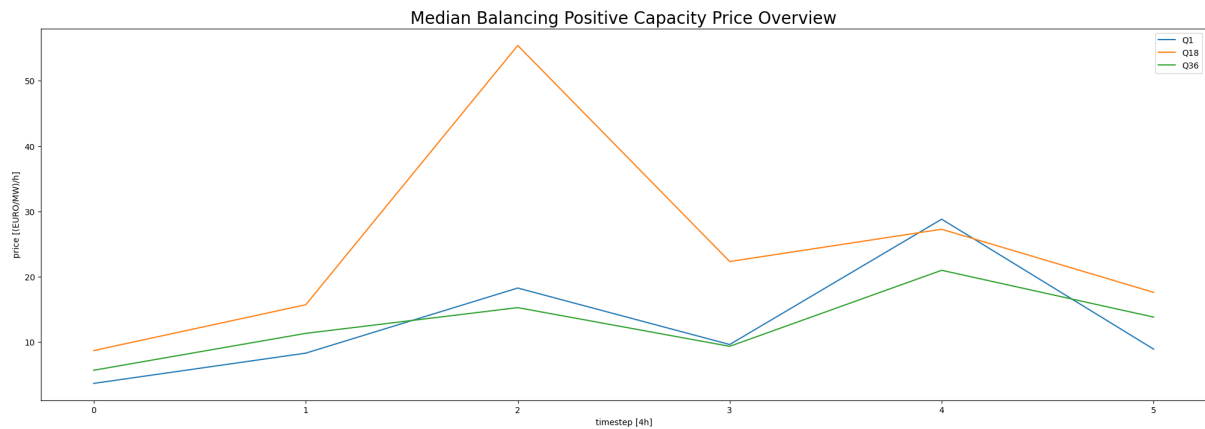


Figure A.16: RL Negative Prices

6.3 Model Results

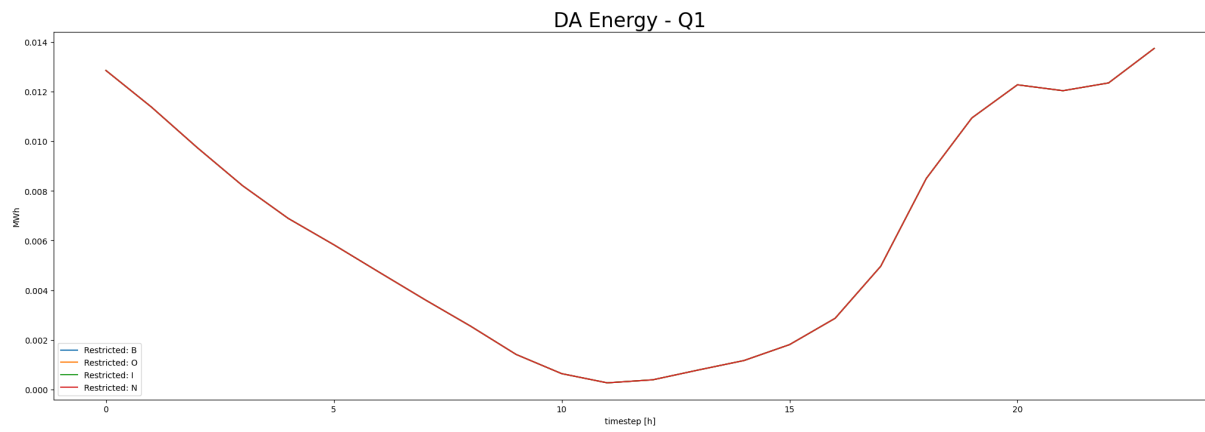


Figure A.17: DA Energy - Q1

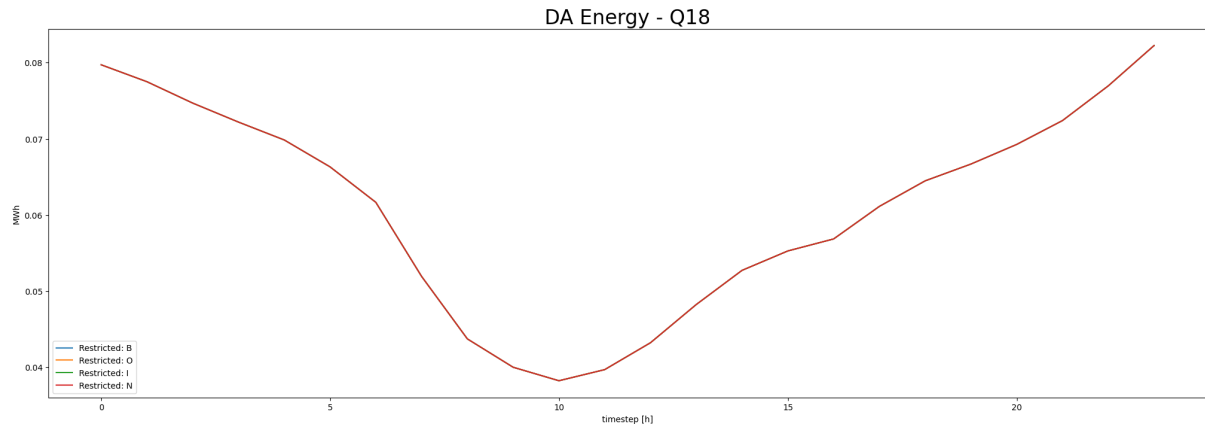


Figure A.18: DA Energy - Q18

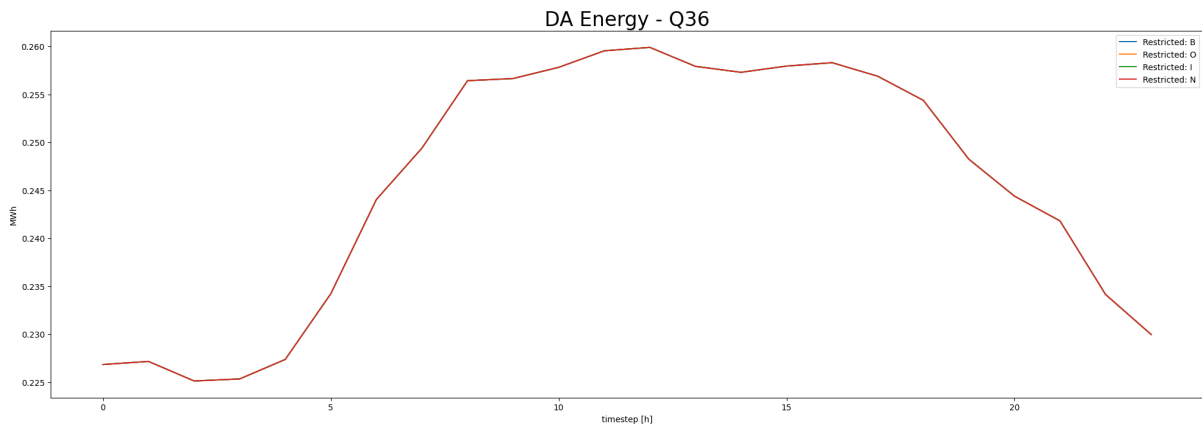


Figure A.19: DA Energy - Q36

6.4 Digital Appendix

6.4.1 Full GAMS Model & Data

Full GAMS Model - Link

https://zenodo.org/records/15250066?token=eyJhbGciOiJIUzUxMiJ9.eyJpZCI6ImQ0YTVlZDAzLWU0NDktNDkyYS1iZGNlLTzMTC3YWNmM2Y3ZCIsImRhGEi0nt9LCJyYW5kb20i0iJhMDh1ZTcwOTU3MjFiZmExMGY0YmUzMjUwZGM2ZjY5ZCJ9.RLOwEcGX1gFzX0IFm-1bEa9GjshtvCu_SmehFOBJg8yQ11NlqWq_4L80uvG4eeULVS_BRhnSywxuA7vsCfTH9w

6.4.2 Python Code, Data & Graphics

Python code for analysis - Link

https://zenodo.org/records/15250072?token=eyJhbGciOiJIUzUxMiJ9.eyJpZCI6ImNmZDY2ZTRmLThiZjctNDI2Yy1hMjkzLWI5NDZkYmVkJMTllNSIsImRhGEi0nt9LCJyYW5kb20i0iJhNjI4MWVmYmJiMGViZTYzOTU0ZDVjMTRmNDU4MWJiMCJ9.uA9bX6OLFf9Pp2ubAHRNnt2GhgJh5wo5rXNe0s0-d_enloZMZBcsV4rCj-NJIkZboyPzi6s5PkMfnyhZUCjNkQ

6.4.3 Alternative Model

Alternative Model - Link

https://zenodo.org/records/15250055?token=eyJhbGciOiJIUzUxMiJ9.eyJpZCI6IjE1YWFjM2QxLWJmOTItNDliOS1iNDY4LWZmODkyNjY10WRiNiIsImRhGEi0nt9LCJyYW5kb20i0iI3ZGI5YjEyODgyNzgxYzdhNGE5Zjc1NWIwOWVhN2YxNSJ9.FBCf0pGd3SIIQKDdfn06Mm0svnNoW9iQm4AwVD-54T6XpgzppI0E8JzMH10q6b0KZh-11kKp2PpRsM_fNMb0nQ

6.4.4 Latex Files

Latex Files - Link

https://zenodo.org/records/15252964?preview=1&token=eyJhbGciOiJIUzUxMiJ9.eyJpZCI6ImZlNjk4YTU4LTMzNTgtNGUyYS05NTIxLTAxZWVkODliZDY0OCIsImRhGEi0nt9LCJyYW5kb20i0iI5NTg4MDU3MDAzzjMzYjM2YjdkMzVhYThiYzVhN2NhMCJ9.QdtnjJpt0wm1z23v3e1TxCvZCGXYiNPDW-LytW3zddZQprKqDhbdlg1VkcCcNoTqt0-4UuMMwPjjLu8F_UjxBGg

Bibliography

- [1] Zhuang Cai et al. 'Optimal Dispatch Scheduling of a Wind-battery-System in German Power Market'. In: *Energy Procedia* 99 (2016), pp. 137–146. ISSN: 1876-6102. DOI: 10.1016/j.egypro.2016.10.105. URL: <https://www.sciencedirect.com/science/article/pii/S1876610216310669>.
- [2] Dheepak Krishnamurthy et al. 'Energy Storage Arbitrage Under Day-Ahead and Real-Time Price Uncertainty'. In: *IEEE Transactions on Power Systems* 33.1 (2018), pp. 84–93. ISSN: 0885-8950. DOI: 10.1109/TPWRS.2017.2685347.
- [3] Christopher Olk, Dirk Uwe Sauer and Michael Merten. 'Bidding strategy for a battery storage in the German secondary balancing power market'. In: 2352-152X 21 (2019), pp. 787–800. ISSN: 2352-152X. DOI: 10.1016/j.est.2019.01.019. URL: <https://www.sciencedirect.com/science/article/pii/S2352152X18303049>.
- [4] Felix Nitsch et al. 'Economic evaluation of battery storage systems bidding on day-ahead and automatic frequency restoration reserves markets'. In: *Applied Energy* 298 (2021), p. 117267. ISSN: 03062619. DOI: 10.1016/j.apenergy.2021.117267.
- [5] Ciaran O'Connor et al. 'Electricity Price Forecasting in the Irish Balancing Market'. In: *Energy Strategy Reviews* 54 (2024), p. 101436. ISSN: 2211-467X. DOI: 10.1016/j.esr.2024.101436.
- [6] 50hertz, amprion, TENNET, TRANSNET BW. 'Modellbeschreibung aFRR-Abrechnung ab 01.10.2021: Modell- & Schnittstellenbeschreibung'. In: (). URL: https://www.regelleistung.net/xspproxy/api/StaticFiles/Regelleistung/Marktinformationen/Modalit%C3%A4ten/_Modalit%C3%A4ten_f%C3%BCr_Regelreserveanbieter_MfRRA/Modellbeschreibung_aFRR-Abrechnung_ab_01.10.2021.pdf.
- [7] 50Hertz Transmission GmbH, Amprion GmbH, TenneT TSO GmbH, ed. *Regelleistung.net*. 18.04.2025. URL: <https://www.regelleistung.net/de-de/>.
- [8] ENTSO-E Transparency Platform. 8.04.2025. URL: <https://transparency.entsoe.eu/>.
- [9] MRL und SRL werden jetzt auf zwei Energiemärkten gehandelt - dem Regelleistungs- und Regelarbeitsmarkt. Erfahren Sie hier mehr über die Details des Regelarbeitsmarkts. 4.12.2024. URL: <https://www.next-kraftwerke.de/wissen/regelarbeitsmarkt>.
- [10] TBATS — sktime documentation. 5.04.2025. URL: https://www.sktime.net/en/latest/api_reference/auto_generated/sktime.forecasting.tbats.TBATS.html.

ChatGPT was utilized in this work for the following purposes:

- As a search tool for specific functions.
- As an aid in refining formulations.

All suggestions were carefully reviewed and assessed individually.

Statement of authorship

I hereby certify that I have authored this document entitled "Model-based analysis of various marketing options on the german secondary balancing market for a large-scale storage facility" independently and without undue assistance from third parties. No other than the resources and references indicated in this document have been used. I have marked both literal and accordingly adopted quotations as such. There were no additional persons involved in the intellectual preparation of the present document. I am aware that violations of this declaration may lead to subsequent withdrawal of the academic degree.

A handwritten signature in black ink, appearing to read "S. Trümper".

Dresden, 20th April 2025

Sebastian Trümper